# AN EXPERIMENTAL STUDY OF BETA-DECAY IN THE LIGHT ELEMENTS

Thesis by

Calvin Wong

In Partial Fulfillment of the Requirements

for the Degree of

Doctor of Philosophy

California Institute of Technology

Pasadena, California

1953

ACKNOWLEDGMENTS

The author wishes to express his indebtedness to Professor C. C. Lauritsen for being allowed to carry on research at the Kellogg Radiation Laboratory. In addition, he wishes to acknowledge the many helpful suggestions and active assistance of Professor T. Lauritsen in connection with the thesis research. He is also indebted to Professors W. A. Fowler and R. F. Christy for valuable advice and consultations.

This work was assisted by the joint program of the Office of Naval Research and the Atomic Energy Commission.

## ABSTRACT

A magnetically compensated stilbene scintillation counter has been developed as a detector for use with a beta-ray lens spectrometer. Reasons for developing such a counter are discussed; design considerations and performance characteristics are given.

The performance of the scintillation counter-lens spectrometer system in the measurement of beta spectra has been investigated. Using the beta spectra of $Na^{22}$ and $P^{32}$, the effects of scattering, source thickness, and source backing upon spectrum shape and end-point have been studied.

The scintillation counter-lens spectrometer system has been employed in studying radioactivity in the light elements. Specifically, the beta-decays of $C^{11}$, $F^{17}$, and $F^{20}$ have been investigated. In the beta-decay of $F^{20}$, the energy discrimination ability of scintillation counters has been employed in investigating the possible existence of a weak high energy beta transition in the presence of a large amount of scattered electrons and room background.

TABLE OF CONTENTS

TABLE OF CONTENTS

# I GENERAL INTRODUCTION

The research embodied in this thesis represents an attempt at a systematic investigation of three beta-decays in the light elements. That such a study is desirable is evidenced by the fact that beta-decay in the light elements has not been investigated as thoroughly or as carefully as in the medium and heavy elements. This unfortunate situation is in large measure attributed to the fact that radioactivity in the light elements is predominantly short-lived, and hence one needs, in addition to a beta-ray spectrometer, a device to induce the radioactivity at the time of measurement. The presence of a 3-Mev Van de Graaf generator and beta-ray spectrometer at the Kellogg Radiation Laboratory thus makes feasible an investigation of beta-decay in the light elements. The ultimate aims of such a study are to determine the decay schemes, and to measure the beta spectra with enough accuracy so that end-point energies and ft-values can be used to predict mass differences and the possible spins and parities of the levels involved in the transitions. In the case of a beta transition to an excited state, the energy of the excited state can be determined through measurements of the delayed gamma radiation. The possible spins and parities of the excited state can be determined from the ft-value of the transition to the excited state.

Although a scintillation counter is not absolutely essential for the study of beta spectra, its versatility and reliability did materially help in determining the beta spectra more accurately. For example, the energy discrimination ability of scintillation counters was employed in discriminating against the low energy machine and room background. The ratio of beta to background counts was improved somewhat with the result that the beta spectra were measured with more reliability. The

scintillation counter is also ideally suited for the detection of weak high energy beta components in the presence of large amounts of low energy background. Such an application is described in the section on the beta-decay of $F^{20}$, in which the ground state transition is highly forbidden. In view of the usefulness of scintillation counters as detectors for beta-ray spectrometers, the design considerations and performance characteristics of such a counter are discussed in some detail in Part II.

A necessary preliminary is the investigation of the performance of the scintillation counter-lens spectrometer system in the measurement of beta spectra. For this purpose, the well-known spectra of $Na^{22}$ and $P^{32}$ were used in studying experimental technique and the method for the analysis of beta spectra. The effects of scattering, source thickness, and backing upon spectrum end-point and spectrum shape have also been studied. These investigations are described in Part III. Finally in Parts IV, V, and VI the investigations on the beta-decay of $C^{11}$, $F^{17}$, and $F^{20}$ are described. Because of time considerations, it was impossible to investigate all the known beta-decays in the light elements. The above three were chosen since the existing experimental evidence on decay schemes and end-point energies was ambiguous.

# II A MAGNETICALLY COMPENSATED STILBENE SCINTILLATION COUNTER

## INTRODUCTION

Almost without exception, beta-ray lens spectrometers utilize end window Geiger counters for the detection of positrons and electrons. Although these counters have a 100% detection efficiency for those electrons and positrons which penetrate the counter window, they do have some undesirable features. End window counters are fragile, and it is difficult to obtain one that is capable of operating reliably for a reasonable length of time. The maximum counting rate possible is limited by the recovery time of the counter. In addition, with a Geiger counter one is not able to discriminate against the low energy room background and low energy electrons scattered into the detector. Since it is known that scintillation counters are capable of high counting rates and of energy discrimination, it was decided to develop such a counter for use with our spectrometer.

Scintillation counters have been adapted to beta-ray lens spectrometers before[1],[2]. However, these adaptations were made chiefly to facilitate pulse height versus electron energy studies for the various scintillation phosphors. Moreover, since the spectrometer utilized in reference (1) contained iron, the magnetic field was confined to the spectrometer proper; the field at the photo-tube was small enough so that magnetic compensation was not required for moderate values of spectrometer current. In our case, even with a 57 cm lucite light pipe, the magnetic field at the photo-tube was 40 gauss for a spectrometer current of 38 amperes. The impossibility of shielding out

such a large field without the use of excessive amounts of iron necessitated the use of magnetic compensation.

## DESIGN CONSIDERATIONS

Since the spectrometer contains no iron, the magnetic field of the spectrometer is directly proportional to the current through its coils. To have compensation at all times, irrespective of the field settings, the compensation current through a suitably designed solenoid must be proportional to the spectrometer current. This was easily accomplished by connecting the compensating coil and a variable series resistance in parallel with the spectrometer coils. This presupposes that the resistance of the spectrometer coils is a constant. This is very nearly true since by means of water cooling the coils are never allowed to heat up excessively.

A measurement of the magnetic field on the axis of the spectrometer at varying distances from its aluminum end plate yielded the following results:

| Distance (cm) | Field (gauss)* |
|---|---|
| 40 | 79 |
| 60 | 36.5 |
| 80 | 18.6 |

As illustrated schematically in Fig. 11, the photo-tube was placed at the end of a 57 cm lucite light pipe. The solenoid, which was 30 cm long, was centered at a distance of 50 cm from the aluminum end plate.

---

* Measurements are for a spectrometer current of 38 amperes.

The solenoid was built to the following design specifications:

| | |
|---|---|
| Length- | 30 cm |
| Diameter- | 8.9 cm |
| Number of layers- | 8 |
| Turns per layer- | 294 |
| Wire size- | B. S. #18, enamel coated |
| Length of wire- | 2140 ft |
| Total resistance- | 14 ohms |

With the above solenoid and a spectrometer current of 38 amperes, the following pertinent quantities were measured or calculated:

| | |
|---|---|
| Voltage across coils- | 40 volts (measured) |
| Field of spectrometer at center of solenoid- | 57 gauss (measured) |
| Resistance in series with solenoid- | 56 ohms |
| Solenoid current- | .575 amp. |
| Total power dissipation- | 23 watts |
| Power dissipated in solenoid- | 4.6 watts |

The success of the design was attested by the fact that the measured value for compensation was .47 amp. as compared with an estimated value of .575 amp. The solenoid was designed with a view towards low power dissipation in it and the accompanying series resistance since it was realized that excessive heating could alter the value of the compensation current. This requirement of low power dissipation was met as

evidenced by the fact that for a spectrometer current of 75 amperes the power dissipation in the solenoid was only 18 watts. In Fig. 12 is presented a drawing of the complete set-up showing the photo-tube, light shield, lucite light pipe, stilbene crystal, and compensating solenoid.

## PERFORMANCE CHARACTERISTICS

In order to set the compensation current to the correct value, the following method was employed: a radioactive gamma-ray source was placed in a fixed position external to the spectrometer proper and the counting rates were observed for different values of the spectrometer current. The compensation current was considered properly set when the counting rates were the same for different values of the spectrometer current between zero and one hundred amperes. When the above procedure was carried out, it was observed that although the compensation was satisfactory for low values of the spectrometer current, the counting rates dropped for currents above 50 amperes, the magnitude of the decrease increasing with increasing currents. This effect implies that the solenoid field does not match the spectrometer field exactly as to magnitude and shape, and that the absolute value of this mismatch increases with increasing currents. To eliminate this difficulty, the photo-tube was surrounded with a shield constructed of mu-metal and transformer iron. The compensation now proved to be satisfactory for currents as high as one hundred amperes.

Having satisfactorily solved the compensation problem, the performance characteristics of the scintillation counter were investigated. The following aspects of the magnetically compensated stilbene scintillation counter were investigated:

(1) Counting efficiency for electrons

(2) Signal to noise ratio

(3) Counter shielding and background counting rates

(4) Counter stability

(5) Maximum counting rate

(6) Effect of energy discrimination upon electrons scattered into the detector

(7) Variation of pulse height output for a given amount of mal-compensation, and

(8) Pulse height versus electron energy relationship.

(1) Counting efficiency for electrons:

By adjusting the spectrometer current to the peak of the 1.32 Mev $Co^{60}$ internal conversion line and comparing the counting rates for a scintillation and Geiger counter, it was found that the counting rates were the same if the scintillation counter was biased on the plateau of the integral bias curve. This therefore indicates that the scintillation counter has a 100% detection efficiency for electrons of this energy.

(2) Signal to noise ratio:

Jentschke et al.[3] have shown that different scintillation phosphors yield different pulse height outputs when struck by monoenergetic electrons. Of the three phosphors investigated by them, NaI yields the greatest pulse height output. But, it was not used in the present investigation because it is hygroscopic. Anthracene is intermediate between NaI and stilbene as regards pulse height output; however, it was not used since large, high quality anthracene crystals are not available commercially. The stilbene crystal used in the present investigation was machined from a larger piece grown in this laboratory

by Mr. Hugh Woodbury. The shape of the machined crystal was a right circular cylinder having a diameter and height of one inch.

Using a stilbene crystal and monoenergetic electrons, it was found that in a batch of six 5819 photo-tubes the signal to noise ratios differed by as much as a factor of three. It was also found that the signal to noise ratio was increased by 50% when the sides as well as one end of the cylindrical stilbene crystal were covered with reflecting aluminum foil. The effect of cooling the photo-tube was investigated. However, the small improvement in the signal to noise ratio did not justify its use. The effect of absorption in the lucite light pipe was also investigated. It was discovered that the signal to noise ratio was reduced by 80% through losses in the light pipe.

Using the best photo-tube, the signal to noise ratio for the final set-up was measured utilizing the Th-B F internal conversion line. The value obtained was 3.2. The procedure followed was to adjust the spectrometer current to the peak of the F-line (147 Kev) and then run an integral bias curve. The signal level is half way up on the integral bias step as shown in Fig. 1.* Since pulse height is linearly proportional to electron energy (see section 8), this indicates that the noise level occurs at an energy corresponding to 47 Kev electrons. Although it is possible to detect electrons with energies as low as 47 Kev, it is not possible to count them with 100% efficiency since the pulse height straggling at these low energies is appreciable. Biasing the scintillation counter at the noise threshold, the F-line (147 Kev) was successfully run with a resolution of 1.99% (see Fig. 2).

---

* The integral bias step is apparent after subtraction of background.

(3) Counter shielding and background counting rates:

The scintillation counter was shielded with lead, cadmium, and paraffin. With the Van de Graaf generator delivering .4 $\mu$a of 2.4 Mev protons, the following background counting rates as a function of counter bias were observed:

| Counter Bias (Mev) | Bkgd. Counts/min. |
|---|---|
| .25 | 520 |
| .50 | 162 |
| 1.00 | 30 |
| 2.00 | 14 |

The counts represent background which is produced when the proton beam strikes brass and tantalum. When running a reaction producing gamma-rays and neutrons, the background is naturally much greater. In any case, the above results indicate that the machine background produces essentially low energy radiation, which can be discriminated against by biasing the scintillation counter as high as possible. Hence the scintillation counter is very effective in discriminating against low energy background.

(4) Counter stability:

The scintillation counter with its associated electronic equipment proved to be quite stable, and hence reliable. Integral bias curves of the Th-D and Th-B internal conversion lines were run daily for four to five days, and each day the pulse heights were reproducible. This also proved to be the case during a day's operation.

(5) Maximum counting rate:

The duration of the light pulses from a stilbene crystal is very short- of the order of $10^{-8}$-$10^{-9}$ seconds. Theoretically then, counting

rates as high as $10^6$-$10^7$ per second are realizable for a 1% counting loss. Practically however, the electronics limit the maximum counting rate realizable for a given counting loss. The scaler utilized decimal counting units manufactured by the Berkeley Scientific Company. The resolving time of these units was 5$\mu$-seconds. Therefore, a counting rate as high as 2000 per second is realizable for a 1% counting loss. In all applications, the counting rates were well below this value, and hence loss corrections were not made.

(6) Effect of energy discrimination upon electrons scattered into the detector:

It has already been demonstrated that energy discrimination is very effective in eliminating counts due to low energy machine background. Therefore, it is evident that the counter would also discriminate against low energy electrons if such were scattered into the detector. However, photo-lines run with a Geiger and scintillation counter yielded almost identical shapes. Hence preliminary evidence seems to indicate that either scattering was not excessive or else the scattered electrons were not much different in energy from the ones being focused* .

(7) Variation of pulse height output for a given amount of mal-compensation:

Because of such effects as resistor heating and aging, it is always possible that the compensation current may change. Therefore it is very important to ascertain how critical compensation is. As a sensitive measure of this, the variation of pulse height output for a

---

* More detailed studies (see Part III) show that the first hypothesis is correct: scattering in the spectrometer is not excessive.

given amount of mal-compensation was determined. Specifically, integral bias curves were run for the Th-D X-line with a ±10% change in compensation current. The results are shown in Fig. 3. Due to shielding, the compensation was not overly critical as a 10% decrease in compensation current reduced the pulse height output by 6.3% while an increase of 10% increased the pulse height output by 2%. These effects are easily explained: increasing the solenoid current focuses electrons in the photo-tube since the solenoid field is mainly axial. On the other hand, decreasing the solenoid current means that part of the spectrometer field at the photo-tube is not being compensated. This field has a large radial component; hence it defocuses electrons in the photo-tube and a decrease in pulse height is observed. Even if a 10% change in current does occur, which is very unlikely, the electrons are still counted with 100% efficiency if the counter is biased sufficiently back on the plateau of the integral bias curve.

(8) Pulse height versus electron energy relationship:

The energy discrimination ability of scintillation counters is based upon the fact that there is a linear relationship between pulse height and energy. This linear relationship certainly holds for scintillation counters without magnetic compensation and without a lucite light pipe, as demonstrated in reference (1). To ascertain if this relationship still holds for a magnetically compensated counter with a lucite light pipe, the pulse height versus electron energy relationship was investigated experimentally. Integral bias curves (Figs. 1, 5-8) were run for the various internal conversion lines*. As shown in these

---

* The integral bias curves all show a sloping plateau. However, if the zero current integral bias curve is subtracted, the plateaus of the resulting integral bias curves are flat within statistics. This fact is illustrated in Fig. 17.

figures, the signal level in arbitrary units is then half way up on the integral bias step. These investigations have shown, as depicted in Fig. 4, that pulse height is directly proportional to electron energy for the range of electron energies employed- namely between 147 Kev and 4.74 Mev. The three upper energy points were obtained from integral bias curves of the $F^{20}$ beta spectrum. These results indicate that the compensation is perfect since the linear relationship is preserved. In addition, they show that the lucite rod absorbs a fixed perdentage of the light produced in the crystal regardless of the electron energy.

Finally, to illustrate the performance and capability of the scintillation counter, the Th-D and Th-B internal conversion lines (4), as run with this counter, are shown in Figs. 2, 9, and 10.

# III THE PERFORMANCE OF THE SCINTILLATION COUNTER-LENS SPECTROMETER SYSTEM IN THE MEASUREMENT OF BETA SPECTRA

## ADJUSTMENTS AND CALIBRATION

The beta-ray lens spectrometer used in the following investigations is fully described in an article by Hornyak, Lauritsen, and Rasmussen [5]. The spectrometer was modified from that described in the paper in two respects: the end window Geiger counter was replaced by a scintillation counter and the spectrometer coils were separated to form a double lens configuration. The geometrical alignment was checked by moving the vacuum chamber with respect to the axis of the coils and observing the intensity of the high energy internal conversion X line of Th-D. The alignment was considered satisfactory when the intensity of the X line was maximized. The compensation for the vertical component of the earth's magnetic field was checked by running the Th-B I and F lines (222 and 147 Kev respectively). The compensation proved to be satisfactory as evidenced by the fact that the resolution for these lines was the same as that for the high energy X line, which would not be the case had the vertical component of the earth's field not been properly compensated. The F, X, and I lines are shown in Figs. 2, 9, and 10. The resolution of the spectrometer was thus about 2%. The effective solid angle was determined to be 2.4% of a sphere. Helical baffles permit observation of electrons and positrons separately.

The spectrometer was calibrated with the Th internal conversion lines. The lines with their corresponding values of momentum in gauss-cm are presented in the following table:

| Line | Gauss - cm |
|---|---|
| Th-D X | $9988.4 \pm 2.0$ [6] |
| Th-B I | $1754.01 \pm 0.25$ [7] |
| Th-B F | $1388.55 \pm 0.20$ [7] |

Several independent determinations of the peak position of these lines were made and then averaged to give the calibration constant. The calibration constants (gauss-cm/milli-volt) for the three manganin shunts used are given in the following table:

| Shunt | Bρ/ M.V. |
|---|---|
| 10 amp. | $42.293 \pm 0.05$ |
| 75 amp. | $159.13 \pm 0.1$ |
| 150 amp. | $317.15 \pm 0.2$ |

For the meaning and significance of the calibration constant, the reader is referred to the article by Hornyak, Lauritsen, and Rasmussen (5).

In all subsequent investigations, the electron or positron detector was a magnetically compensated stilbene scintillation counter. The compensation was checked periodically by placing a gamma-ray source in a fixed position external to the spectrometer proper and observing the counting rates as a function of spectrometer current. Even for the highest currents utilized in any of the given experiments, the counting rates were constant, showing that the counter sensitivity was not a function of spectrometer current. In addition to checking the compensation, the scintillation counter itself was checked at the beginning of a day's run with a gamma-ray source placed in a fixed position. Integral bias curves, at different electron energies, were run periodically to check that the counter was operating satisfactorily.

The counter proved to be quite stable as pulse height output for a given electron energy was reproducible over a period of several months. This fact implies the use of a fixed value for the high voltage on the 5819 photo-tube; the particular value chosen was 800 volts.

## THE BETA SPECTRA OF $Na^{22}$ AND $P^{32}$

Since $Na^{22}$ and $P^{32}$ are relatively long-lived and easily available, they are ideally suited for checking the performance of the scintillation counter-lens spectrometer system in the measurement of positron and electron spectra. Since the end-point energies and spectrum shapes are well-known, they can also be used to check such items as scattering, and effects of source thickness and source backing. In addition, the accurately known end-point energies will provide a check on experimental technique, and on the method in which the data is analyzed to construct a Fermi-Kurie plot.

The $Na^{22}$ ($\tau_{\frac{1}{2}}$= 2.6 years) was in the form of a solid salt of sodium. The source was prepared by sandwiching a small quantity of the salt between scotch tape and $\frac{1}{4}$ mil aluminum foil. The energy loss of the positrons in the foil (1.7 mg/cm$^2$ thickness) is estimated to be of the order of two to three Kev at most. The positron spectrum has been investigated by Macklin, Lidofsky, and Wu[8]. They find that the Fermi-Kurie plot is linear down to 25 Kev, and that the spectrum end-point is 542±5 Kev. The experimentally observed momentum spectrum is shown in Fig. 13.

The $P^{32}$($\tau_{\frac{1}{2}}$= 14.1 days) was in the form of a solution of a salt of phosphorus. The source was prepared by placing a drop of the solution on 0.15 mil aluminum, and then heating to drive off the solvent. The electron spectrum has been studied by many investigators. The various

determinations of the end-point energy are summarized in reference (9). The weighted mean of all the measurements indicates that the end-point is $1.707 \pm 0.004$ Mev[9]. The Fermi-Kurie plot is linear down to at least 260 Kev[10]. The experimentally observed spectrum is shown in Fig. 15.

## METHOD OF ANALYSIS OF BETA SPECTRA

The $Na^{22}$ and $P^{32}$ beta spectra (Figs. 13, 15) were analyzed by extending the background tail to lower energies (see Fig. 15) and subtracting the extrapolated background from the recorded counts at each point. The major part of the extrapolated background is the constant room background. However, because the background tail does slope somewhat, the net effect is that an extrapolated straight line gives more background counts at the low energy end of the beta spectrum. This method of background subtraction, although questionable, is at least qualitatively correct since one would expect more scattering the lower the energy of the beta-rays. Since the slope of the background tail is so slight, the assumption of a constant background for the spectrum should yield about the same end-point. This point was checked by calculations on the $P^{32}$ beta spectrum: assumption of either the constant room background or the slightly sloping background gave the same end-point to within one Kev. A constant background gave 1.711 Mev while a sloping background gave 1.712 Mev by least squares analysis.

The number of beta counts per unit momentum interval was obtained by dividing the observed counts, corrected for background, by the "Window" of the spectrometer at the given momentum setting. The other alternative is to "unfold" the observed momentum spectrum with the spectrometer resolution curve to obtain the true spectrum. Analyzing

the $Na^{22}$ and $P^{32}$ by dividing the observed counts by the momentum window gave straight line Fermi-Kurie plots (Figs. 14, 16) and the correct end-points. Hence the more laborious method of "unfolding" can be dispensed with. The values of the Fermi function used in constructing the Fermi-Kurie plots were obtained from "Tables for the Analysis of Beta Spectra" published by the National Bureau of Standards. In all cases, corrections have been applied for the effects of screening by the atomic electrons. These corrections are also given in the above tables.

Fig. 14 shows the resulting Fermi-Kurie plot for $Na^{22}$. The 540 Kev end-point* is in agreement with the work of Macklin, Lidofsky, and Wu[8] . The Fermi-Kurie plot is linear down to 200 Kev, the lowest energy at which the spectrum was measured.

Fig. 16 shows the Fermi-Kurie plot for $P^{32}$. The end-point of 1.711 Mev is in agreement with the weighted mean of all the other measurements[9] . The Fermi-Kurie plot is linear down to 330 Kev, the lowest energy at which the spectrum was measured.

The above procedures and techniques, having been tested on the $Na^{22}$ and $P^{32}$ and found adequate, have been applied in the analysis of all subsequently measured beta spectra.

## EXTENT AND EFFECT OF SCATTERING

Scattering potentially has the greatest effect in producing false end-points and distorted spectra. For this reason, the extent and

---

* The quoted end-point includes a 3 Kev correction for energy loss in the aluminum foil.

effect of scattering in the spectrometer have been investigated in some detail. That some degree of scattering is present is evidenced by the very slight tail observed beyond the end-point in both the $Na^{22}$ and $P^{32}$ momentum plots, Figs. 13, 15 respectively*. By tail is meant the counts remaining beyond the end-point of the beta spectrum after the constant room background is subtracted. The magnitude of this tail is quite small, being a few tenths of a percent of the peak of the beta spectrum. For the $Na^{22}$ the figure is 0.5%, while for the $P^{32}$ it is 0.25%**. This tail extends about 10% beyond the end-point, and eventually it runs into the zero current or room background. The magnitude of the measured room background is of course dependent upon how low the counter bias is. For example, in the case of the $Na^{22}$ momentum spectrum the measured room background amounted to 135 counts per minute. The corresponding bias was such that 200 Kev electrons were counted with 100% efficiency. In the case of the $P^{32}$, the measured room background was 88 counts per minute. The background was lower since the counter was biased so as to count 500 Kev electrons with 100% efficiency. The measurement of the $P^{32}$ spectrum below 500 Kev involved a change of bias to a lower value.

The fact that the assumption of a constant room background for the entire $P^{32}$ spectrum gave the correct spectrum shape and end-point implies that the scattering at different points of the beta spectrum cannot be excessive. The amount of scattering at different points of

---

* Hornyak and Lauritsen (11) in measurements on the $N^{13}$ beta spectrum observed a similar field sensitive background.

** This discrepancy can be accounted for by the poor statistics (see Figs. 13, 15); it cannot be accounted for by the high energy beta-rays from $Na^{22}$ since the ground state branching ratio is only 0.06% (12).

the beta spectrum was investigated by running integral bias curves. If scattering were excessive, the plateaus of the integral bias curves should show a noticeable rise as the bias is lowered. This effect has been observed near the end of a beta spectrum where the number of scattered electrons is comparable to that of direct electrons. Experimentally it is observed that if the zero current integral bias curve is subtracted from the observed integral bias curves, the plateaus of the resulting integral bias curves at different points of the beta spectrum are flat within statistics. This fact is illustrated in Fig. 17, which represents integral bias curves taken at different points of the $P^{32}$ beta spectrum.

The effect of counter bias upon measured spectrum end-point has also been investigated. The $P^{32}$ beta spectrum was run with two different biases. It was observed that, within statistics, the two curves are identical if a correction is made for the increase of recorded room background counts with lower bias. This again indicates that the scattering at different points of the beta spectrum cannot be excessive. If scattering were serious, then a lowered bias would record the low energy scattered electrons, and the spectrum would deviate from that observed with a higher bias.

The conclusion is therefore that a small degree of scattering is present. However, the number of scattered counts at a given point of the beta spectrum is of the order of the statistical variation of measured counts at that point, and hence scattering has a negligible effect on spectrum shape and end-point.

Finally, the most effective argument for negligible scattering is the fact that measurements on $Na^{22}$ and $P^{32}$ gave the correct end-points

and straight line Fermi-Kurie plots down to 200 and 330 Kev respectively.

## EFFECT OF SOURCE THICKNESS

It is not entirely clear how the end-point is shifted or how the spectrum is distorted if the beta-rays traverse a finite thickness of material. The effect of source thickness upon spectrum shape and end-point has been experimentally investigated utilizing the beta spectrum of $P^{32}$. The source was deposited on a quartz film of measured thickness 4.7 mg/cm$^2$ . The spectrum was first measured with the electrons traversing zero thickness and then with the electrons traversing a thickness equal to 4.7 mg/cm$^2$ . Since it was realized that the shift is quite small- of the order of 6-7 Kev - the spectrum in the two cases was carefully measured. The statistics at all points except those close to the end-point were good to 1%, which is equivalent to 10,000 counts at each point. The respective measured spectra are shown in Fig. 18. The dots correspond to the 4.7 mg/cm$^2$ beta spectrum curve. By inspection, it is seen that the 4.7 mg/cm$^2$ curve is shifted bodily to a lower energy.

Construction of Fermi-Kurie plots (Figs. 19, 20) for the two cases shows that a thickness of 4.7 mg/cm$^2$ reduces the measured beta spectrum end-point by 8 Kev. (The end-points were obtained by a least squares analysis of the two sets of data.) This figure is reasonable since electrons, on the average, lose about 1.5 Kev/mg/cm$^2$ if the electron energy is greater than 400 Kev. Having determined the shift for a given thickness, empirical corrections can now be applied to those cases where the beta-rays traverse a given foil thickness. In addition, the Fermi-Kurie plot of Fig. 20 yields a straight line. This fact indicates that a

source thickness as great as 4.7 mg/cm$^2$ produces no serious distortion of the beta spectrum down to at least 330 Kev.

## EFFECT OF SOURCE BACKING

By running the $P^{32}$ beta spectrum with different thicknesses of backing material, the effect of source backing upon spectrum end-point and shape was investigated. The spectra run with backing thicknesses of 1 and 4.7 mg/cm$^2$ are shown in Figs. 15, 18 (solid curve) respectively. The Fermi-Kurie plots of the corresponding spectra, Figs. 16, 19 respectively, show that the end-point is not affected by backing thickness as would be expected. The two end-points, determined by least squares analysis, differed by one Kev. In addition, Fig. 19 shows that a backing thickness as great as 4.7 mg/cm$^2$ produces no observable distortion of the beta spectrum down to at least 330 Kev.

# IV THE BETA-DECAY OF $C^{11}$

## INTRODUCTION

$C^{11}$ is a positron emitter with a half-life of 20.4 minutes[13]. It provides an example of a superallowed beta transition since the daughter nucleus, $B^{11}$, is the mirror of $C^{11}$. It is therefore expected that the spectrum is simple, the beta-decay going predominantly to the ground state of $B^{11}$. The spectrum was measured by Townsend[14], and Siegbahn and Bohr[15]. They found the beta spectrum to be simple. In addition, Siegbahn and Peterson[16] observed the absence of $\gamma$-$\gamma$ coincidences*. The end-point determinations were: Townsend, $0.981 \pm 0.005$ Mev; Siegbahn and Bohr, $0.993 \pm 0.01$ Mev. The main reason for remeasuring the $C^{11}$ positron spectrum is that the above reported beta-ray end-point energies are considerably higher than that expected from the $B^{11}(pn)\ C^{11}$ threshold measurement. The threshold measurement reported by Richards and Smith[17] predicts a beta-ray end-point of $0.958 \pm 0.003$ Mev. The discrepancies thus lie outside the combined probable errors.

## EXPERIMENTAL METHOD

Radioactive $C^{11}$ was produced by the $B^{10}(dn)C^{11}$ reaction. The target assembly consisted of a thin layer of $B_2O_3$ (normal $B^{10}$ abundance) melted onto an 0.15 mil aluminum foil. This foil was then fastened to a 4 mil supporting aluminum foil which had a 3/8 inch hole in its center.

---

* They looked for coincidences between annihilation radiation and gamma-rays.

Since the production of $F^{17}$ positrons would interfere with the beta spectrum measurements, the target was bombarded with 1.77 Mev deuterons. The bombarding energy is below the $O^{16}(dn)F^{17}$ threshold at 1.836 Mev[18]. A bombardment of 20 minutes with a beam current of 0.5 $\mu$a was sufficient to produce a usable activity. At the end of the bombardment, the accelerator was shut down and the target was reversed before counting commenced. Reversal of the target means that the bombarded $B_2O_3$ now faced the scintillation counter end of the spectrometer so that the majority of the positrons traversed zero source thickness. The spectrum was normalized by referring all points to a fixed point in the spectrum. Each point in the spectrum was determined by the following procedure: at a particular field setting, counts were recorded for one minute. The counter was then turned off for one minute, during which time the spectrometer current was changed back to the reference field setting. The counts at the reference setting were then also measured for one minute. Although the accurately known half-life could be used for normalization purposes, it was felt that the above more tedious procedure was more accurate since the counts at each point were directly compared with the number of counts at the reference point of the beta spectrum. Counting was carried out over one half-life or 20 minutes, in which time 5 points could be determined. During each counting interval, the half-life was carefully checked. In all cases, the counting rate does drop to half-value in 20 minutes. This agreement with the known half-life provides an added check that the positrons being counted are from the $C^{11}$. The turning on and off of the counters for 1 minute intervals was accomplished by a set of relays actuated by a synchronous motor.

## POSITRON SPECTRUM

The observed momentum spectrum is shown in Fig. 21. Beyond the end-point a slightly sloping background is again observed. This tail is well understood from studies of the $Na^{22}$ and $P^{32}$ beta spectra. Subtracting the background and making the usual Fermi-Kurie plot yields the straight line of Fig. 22. An average of three determinations gave an end-point energy of 970 ± 8 Kev*. A least squares analysis was also made for one of the three sets of data; the graphical and least squares solutions agreed to within two Kev. Fig. 22 shows that a straight line fits the Fermi-Kurie plot down to at least 255 Kev. The measurements were not carried below this value since the background correction, resulting from the lowered bias, was appreciable.

## DISCUSSION

The end-point energy of 970 Kev coupled with a half-life of 20.4 minutes gives an ft-value of 4170 seconds. Hence the ft-value confirms the fact that the transition is superallowed since $C^{11}$ and $B^{11}$ are mirror nuclei. The ft-value lies within the accepted range for mirror transitions: ft between 1000-5000 seconds.

Examination of the level scheme for $B^{11}$ reveals that the possibility of a delayed gamma-ray being associated with the beta-decay is definitely ruled out by energy considerations: the first excited state of $B^{11}$ has an excitation energy of 2.14 Mev above the ground state.

The end-point determination lies between the previously measured

---

* Includes a 1 Kev correction for source thickness.

end-points[14],[15] and that predicted from the threshold measurement. The combined probable errors overlap in all cases with the exception of the end-point reported by Siegbahn and Bohr[15]. The present results therefore do not indicate whether the previous beta-ray or threshold measurement lies closer to the truth.

# V THE BETA-DECAY OF $F^{17}$

## INTRODUCTION

The ground and excited states of the mirror nuclei $O^{17}$ and $F^{17}$ have been extensively investigated[19]. It has been generally concluded that the ground and first excited states of these nuclei have spins and parities given by $J = 5/2 +$ and $J = 1/2 +$ respectively (see Fig.26). Since $O^{16}$ has spin zero and even parity and represents the closure of the p-shell, this would indicate on the shell model that the extra neutron or proton outside the closed shell has the $\ell$-values 2 and 0 respectively.

$F^{17}$ is unstable for positron emission to $O^{17}$. The reaction $F^{17}(\beta^+)\ O^{17}$ has been known for a long time[20] ; in fact a standard way of detecting the capture of protons by $O^{16}$ is by observing the decay positrons of the $F^{17}$. Previous investigators[21] observed an excess of positrons at the low energy end of the beta spectrum. This was interpreted by Bethe, Hoyle, and Peierls[22] to mean that the actual spectrum was complex with a low energy component going to an excited state of $O^{17}$ . This supposition was apparently confirmed by V. Perez-Mendez and P. Lindenfeld[23] whose work indicated that the spectrum was complex with two components of maximum energy 1.72 and .78 Mev respectively. The ft-values of the high and low energy components were respectively 3240 and 350 seconds. In addition, a gamma-ray of energy $.98 \pm .05$ Mev ($\tau_{\frac{1}{2}} = 70$ sec.) was observed.

An allowed ft-value of 3240 seconds for the ground state transition is in agreement with the theory of mirror nuclei. The ground state transition is $\Delta J = 0$; no, and hence allowed on either the Gamow-

Teller or Fermi selection rules. However, an ft-value of 350 seconds for the excited state transition is unexpectedly small. For this case, the assignment of spins and parities discussed above predicts according to either the Fermi or Gamow-Teller selection rules a second-forbidden transition, with a spin change of two units and no change in parity. Thus a much larger ft-value than that reported in reference (23) would be expected.

A later publication by Perez-Mendez and Lindenfeld[24] reported that the originally observed gamma-ray does not exist. In view of this result, it may be concluded that the beta spectrum is simple, and the contradiction discussed in the previous paragraph is removed. Since however, the beta spectrum has not been remeasured, it was thought worthwhile to reinvestigate the positron spectrum in order to check the linearity of the Fermi-Kurie plot and in order to determine more accurately its end-point. For the sake of completeness, a search for delayed gamma radiation following the beta-decay was also made.

## SEARCH FOR DELAYED GAMMA RADIATION

A careful search was made for 874 Kev delayed gamma radiation. This radiation is emitted if the beta-decay has a branch proceeding to the first excited state of $O^{17}$. The search was made with both the lens and scintillation spectrometers. In the scintillation spectrometer studies, the deuteron beam struck a thick quartz slab mounted within an evacuated target chamber. In the lens spectrometer studies, the deuteron beam was brought directly into the vacuum chamber of the spectrometer in order to bombard a quartz target at the source position.

In the lens spectrometer search, the target assembly consisted of a 31 mil quartz ($SiO_2$) slab, 100 mil aluminum absorber, and 23.2 mg/cm$^2$

thorium converter. Before an effective search can be made, it is necessary that the shape of the photo-peak and Compton edge for an 874 Kev gamma-ray be accurately known. To this end, the 874 Kev prompt gamma-ray from the $O^{16}(dp)O^{17*}$ reaction was measured with the above target assembly. The deuteron bombarding energy was 1.77 Mev, which is below the $O^{16}(dn)F^{17}$ threshold at 1.836 Mev[18]. The observed conversion spectrum from the 874 Kev prompt gamma-ray is shown in Fig. 23 (dotted curve). The spectrum was normalized by monitoring the prompt gamma-rays with a Geiger monitor. The position of the K photo-peak yielded an energy of 872 Kev for the gamma-ray energy, in agreement with the results of Thomas and Lauritsen[25].

In the search for the delayed gamma-ray following the $F^{17}$ beta-decay, the region of the 874 Kev K photo-peak was surveyed with the lens spectrometer. To show that positrons were being produced and to check the method of normalization, the K photo-peak from the annihilation radiation was also measured. The results are shown in Fig. 23 (circled curve). The position of the K photo-peak yielded an energy of 507 Kev for the annihilation radiation. The agreement is satisfactory in view of the fact that the photo-peak was not determined with a high degree of precision. The asymmetry of the photo-peak is caused by the fact that for annihilation radiation a 23.2 $mg/cm^2$ thickness of thorium amounts to a thick photo-electric converter. This point is discussed fully in the article by Hornyak, Lauritsen, and Rasmussen[5].

The procedure followed in obtaining the delayed spectrum was to bombard the target with 1 $\mu$a of 2.32 Mev deuterons for two minutes with the detector and monitor turned off. In order to avoid counting

the intense prompt radiation, the high voltage on the Geiger monitor was reduced to below the threshold value during the bombardment period. At the end of the bombardment period, the voltage on the electrostatic generator was turned down mainly to reduce the background counting rates for both the detector and monitor counters. An additional 25 seconds was introduced between the end of the bombardment and the turning on of both counters in order to allow the $P^{29}$ activity ($\tau_{\frac{1}{2}} = 4.6$ seconds) to decay. The detector reading was normalized to a fixed monitor reading. The monitor counter recorded the annihilation radiation from the target, and counting was carried on for 90 seconds, or approximately 1.5 $F^{17}$ half-lives.

In Fig. 23, the conversion electrons from the prompt and delayed radiation as measured with the lens spectrometer are shown. The prompt radiation spectrum (dots) displays the usual Compton edge, K, and L photo-peaks from conversion processes while the corresponding delayed radiation spectrum (circles) displays no such structure. This then indicates the absence of 874 Kev delayed gamma radiation. Consequently, it can be said that the beta-decay of $F^{17}$ shows no visible branching to the known 874 Kev level in $O^{17}$. From the Geiger monitor readings and the areas of the K photo-peaks, the yield of positrons and prompt gamma-rays was calculated. Both methods gave essentially the same answers: the prompt radiation spectrum corresponded to the production of $2.1 \times 10^9$ 874 Kev quanta; the delayed spectrum corresponded to the production of $1.0 \times 10^{9*}$ positrons. The

---

* Measurements indicate that, at most, 2% of these positrons are from the $P^{30}$. This figure is very nearly equal to the ratio of the abundances of $Si^{29}$ to $O^{16}$ in quartz. Since the statistical variation of Geiger monitor counts amounted to about 3%, the effects of the $P^{30}$ positrons can be neglected.

dashed curve of Fig. 23 corresponds to the expected K photo-peak if all the positrons went to the 874 Kev level in $O^{17}$. The delayed spectrum in the region of the 874 Kev K photo-peak is essentially flat. The observed scattering of points can be fully accounted for by the statistics. Hence the statistical variation of counts sets an upper limit upon the possible existence of an 874 Kev delayed K photo-peak. From the statistics, it is concluded that in the beta-decay of $F^{17}$ less than 2% of the beta transitions result in 874 Kev delayed gamma radiation. This estimate is consistent with a later one based upon an examination of the Fermi-Kurie plot.

The search for the delayed gamma-ray was also made with the more sensitive techniques of scintillation spectroscopy since it is known that a scintillation counter can detect a gamma ray whose intensity is an order of magnitude weaker than that which can be detected by a lens spectrometer. The light pulses from a NaI scintillation counter were displayed on an oscilloscope and photographed. Photographs of the delayed gamma radiation spectrum revealed, however, a gamma-ray whose energy was considerablyhigherthan 874 Kev. By direct comparison with the $Na^{22}$ $\gamma$-ray ($E\gamma$ = 1.275 Mev), the energy of this delayed gamma-ray was determined to be $1.32 \pm 0.07$ Mev. The half-life of this gamma-ray was observed to be much shorter than the $F^{17}$ half-life of 66 seconds, since this activity disappeared completely in a time comparable to the $F^{17}$ half-life. By allowing the short-lived activity to decay, a search was then made for 874 Kev delayed $\gamma$-radiation presumably associated with the beta-decay of $F^{17}$. The scintillation spectrometer was calibrated with the 874 Kev prompt gamma-ray from the $O^{16}(dp)O^{17*}$ reaction. In all photographs, intense annihilation radiation was observed, but no indications were found for the existence of 874 Kev

delayed gamma radiation. This result is in accord with that obtained by W. E. Myerhof[26] of Stanford who reports "....in the beta-decay of $F^{17}$ less than 1 percent of the beta transitions result in gamma radiation."

The assignment of the 1.32 Mev delayed gamma-ray to the beta-decay of $P^{29}$ is based on the work of Roderick, Lönsjö, and Meyerhof[27] who report the beta-decay of $P^{29}$ shows branching to excited levels of $Si^{29}$ at 1.28 and 2.43 Mev. There were also indications in the scintillation spectrometer studies for the presence of a 2.43 Mev delayed gamma-ray, but quantitative measurements of energy were not made. This assignment of the 1.32 Mev delayed $\gamma$-ray is plausible since in the course of work done with quartz targets the $P^{29}$ activity[28] was actually identified by rough energy and half-life measurements: the end-point energy was roughly $3.8 \pm 0.2$ Mev, and the half-life was approximately 5 seconds. The production of $P^{29}$ is energetically possible since the $Si^{28}(dn)P^{29}$ reaction has a Q-value of $0.29 \pm 0.04$ Mev[29].

## POSITRON SPECTRUM

The first attempts at measurement were made employing 3/4 mil quartz films. These measurements were unsatisfactory because two additional activities were found to be present. These activities were positrons from $P^{29}$ and $P^{30}$, produced by (dn) reactions on $Si^{28}$ and $Si^{29}$ [29] respectively. The $P^{30}$ activity was identified only through a half-life determination of roughly 2.4 minutes. PbO targets evaporated on 0.15 mil aluminum foils proved to be quite satisfactory, as no activity other than the 66 second $F^{17}$ activity was observed. These targets were supported by 3 mil aluminum foils which had 3/8" holes in

their centers; these were used in all subsequent beta spectra measurements.

The problem of normalizing the different points in the positron spectrum turned out to be quite troublesome. It is true that annihilation radiation is present, but this originates mainly from positrons being stopped in the spectrometer walls since the targets are thin, and since the positrons are bent by the magnetic field it is conceivable that the amount of annihilation radiation as seen by the monitor counter is a function of spectrometer current*. In the absence of any other simple normalization methods, the spectrum was normalized by referring all measurements to one point in the spectrum. Each point in the spectrum was determined by the following procedure: at a particular field setting counts were recorded for 30 seconds. The counter was then turned off for 30 seconds, during which the spectrometer current was changed back to the reference field setting. Finally, counts at the reference setting were recorded for 30 seconds. This method has the advantage that the normalization does not depend upon the half-life of the decay. The counter was turned on and off for 30 second intervals by means of relays actuated by a synchronous motor.

---

* This difficulty does not appear when normalizing the delayed gamma radiation spectrum. In this case, half of the positrons produced near the outer surface of the quartz target is stopped by the 31 mil quartz slab and 100 mil aluminum absorber. The number of annihilation quanta from the target assembly is thus equal to the number of positrons produced. The remaining positrons being stopped in the spectrometer walls give rise to a diffuse source of annihilation radiation. This latter radiation does not contribute appreciably to the monitor counting rate as the monitor is shielded with lead in such a manner as to accept only radiation from the direction of the target assembly.

The bombardment time was of the order of 2 minutes, at the end of which the voltage on the electrostatic generator was turned down before the counting interval started, mainly to reduce the background counting rate.

The observed momentum spectrum is shown in Fig. 24. Beyond the end-point, a gradual decrease in the background with increasing field is discernable. Eventually the background runs into the zero current or room background. The same sort of phenomenon is observed in the momentum spectra of $Na^{22}$ and $P^{32}$, and is to be attributed to the small degree of scattering present in the spectrometer. This point has been adequately discussed in section III and need not be entered into here.

Subtracting the background and making the usual Fermi-Kurie plot for $F^{17}$ yielded the straight line of Fig. 25. An average of three determinations yielded an end-point energy of $1.749 \pm 0.006$ Mev. This is in agreement with the results of V. Perez-Mendez and P. Lindenfeld [23] who report the end-point energy as $1.72 \pm 0.03$ Mev. A least squares analysis was also made of the three sets of data, and it was discovered that the graphical and least squares solutions agree to within 2 Kev.

The Fermi-Kurie plot is linear from the end-point on down to an energy of around 500 Kev, which is the lowest energy at which the spectrum was measured. If the spectrum were complex, a deviation from linearity should occur at around 875 Kev. Since this is not observed experimentally, it is concluded that the beta spectrum consists of only one component. The deviation from linearity observed in reference (23) at around 775 Kev is presumably due to scattered positrons caused

by excessive source thickness.

## DISCUSSION

The present investigation shows the absence of any 874 Kev delayed gamma radiation associated with the beta-decay of $F^{17}$. The lens spectrometer studies indicated an upper limit of 2% for the excited state branching ratio. This is in agreement with the results obtained in references (24) and (26).

Deuteron bombardment of quartz ($SiO_2$) targets reveals, in addition to the $F^{17}$ activity, the presence of $P^{29}$ and $P^{30}$ positron activity. The assignment of the $1.32 \pm 0.07$ Mev delayed gamma-ray to the beta-decay of $P^{29}$ is based mainly upon the work of Roderick, Lönsjö, and Meyerhof[27].

The beta spectrum consists of one component of maximum energy $1.749 \pm 0.006$ Mev. This value is in agreement with that calculated by Li[9] as $1.745 \pm 0.006$ Mev. The calculation is based on the threshold measurement for the $O^{16}(dn)F^{17}$ reaction, as well as the Q-value for the $O^{16}(dp)O^{17}$ reaction.

The beta spectrum is of the allowed shape: a straight line fits the Fermi-Kurie plot from the end-point on down to 500 Kev. From an examination of the Fermi-Kurie plot, an upper limit can be put on the transition to the known 874 Kev level in $O^{17}$. If the excited state transition does occur, its intensity is less than 1 percent of the ground state transition. This result is again in agreement with the result of W. E. Meyerhof[26].

The experimentally determined half-life was $66.0 \pm 1.8$ seconds. This value coupled with the end-point determination gives an ft-value

of 2420 seconds for the ground state transition. This transition then belongs to the class of so-called "superallowed" of "Wigner" transitions where the ft-values lie between 1000-5000 seconds. "Superallowed" transitions are transitions between states whose wave functions are very similar. This is precisely what one would expect since the transition occurs between the ground states of two mirror nuclei, $F^{17}$ and $O^{17}$.

The minimum ft-value for the excited state transition is $2 \times 10^4$ seconds, i.e. ft $\geq 2 \times 10^4$ seconds and is probably much greater. This is reasonable since the assignment of spins and parities to the levels predicts a second-forbidden transition (ft of the order of $10^{13}$ seconds)[30].

## SUMMARY

The $F^{17}$ $(\beta^+)O^{17}$ reaction has been investigated with a magnetic lens spectrometer employing sources activated by the $O^{16}(dn)F^{17}$ reaction. The positron spectrum of $F^{17}$ consists of one component of maximum energy $1.749 \pm 0.006$ Mev. The Fermi-Kurie plot is linear from the end-point down to 500 kev. Beta-ray branching to the first excited state of $O^{17}$ at 874 Kev, if present, is estimated to have a relative intensity of $<1\%$ of the ground state transition. This estimate is consistent with the failure to observe any 874 Kev delayed gamma radiation in conjunction with the annihilation radiation. The lens spectrometer studies indicated an upper limit of 2% for the excited state branching ratio. The ft-value for the ground state transition is 2420 seconds, while the minimum ft-value for the excited state transition is $2 \times 10^4$ seconds.

The search for delayed gamma radiation, which was made employing quartz ($SiO_2$) targets, reveals however the existence of a $1.32 \pm 0.07$ Mev delayed gamma-ray. The assignment of this gamma-ray to the beta-decay of $P^{29}$, produced by the $Si^{28}(dn)P^{29}$ reaction, is based mainly upon the work of Roderick, Lönsjö, and Meyerhof[27].

# VI THE BETA-DECAY OF $F^{20}$

## INTRODUCTION

Previous investigators[31],[32] have shown that the main body of the beta-decay of $F^{20}$ proceeded to an excited state of $Ne^{20}$ with the subsequent emission of 1.63 Mev gamma radiation. However, there was no general agreement as to the end-point energy of the intense beta component, nor as to the complexity of the electron and the delayed gamma radiation spectrum. It was primarily in the interest of clarifying these points that the present investigation was undertaken.

After the investigation was begun, it was learned that D. E. Alburger at Brookhaven had worked on the same problem. His results, then communicated prior to publication but now recently published[33], did not agree with either Jelley or Littauer. The results of the present investigation however, confirm those obtained by Alburger.

The conflicting results of Jelley, Littauer, and Alburger are summarized below:

Jelley [31] finds the gamma-ray spectrum to be complex: the gamma radiation consists of two components of energy $1.64 \pm 0.05$ and $2.45 \pm 0.06$ Mev, having an intensity ratio of 8.4 to 1. The beta spectrum is composed of one component of maximum energy $5.03 \pm 0.05$ Mev.

Littauer[32] finds that the gamma-ray spectrum is probably complex. He observes a strong gamma-ray of energy $1.63 \pm 0.02$ Mev, which is associated with the main body of the $F^{20}$ beta-decay. In addition, he observes a weak 1 Mev gamma-ray whose allocation to the $F^{20}$ beta-decay cannot be excluded. The 2.45 Mev gamma-ray reported by Jelley is not observed. The electron spectrum is complex in that 3.5 percent of the

transitions occur directly to the ground state: $E_\beta$ (max) = 6.74 ± 0.1 Mev. The more intense beta group has an end-point energy of 5.33 ± 0.05 Mev.

Alburger[33] finds both the beta and gamma spectrum to be simple. The electron spectrum consists of one component of maximum energy 5.406 ± 0.017 Mev. The beta-decay proceeds to an excited state of $Ne^{20}$ which decays by the emission of 1.631 ± 0.006 Mev gamma radiation. Beta-ray branching to the ground state of $Ne^{20}$, if present, has a relative intensity of less than 1 percent. The 1 and 2.45 Mev gamma-rays observed by Littauer and Jelley respectively are not observed.

In addition to clarifying the decay scheme, the present investigation was undertaken for the purpose of determining accurately the $F^{20}$ - $Ne^{20}$ atomic mass difference. This mass difference, in conjunction with the Q-values for the reactions $Ne^{20}(dp)Ne^{21}$, Q = 4.529 ± 0.007 Mev[34] ; and $F^{19}(dp)F^{20}$, Q = 4.373 ± 0.007 Mev[35] , can be used to predict the Q-value for the $Ne^{21}(d\alpha)$ $F^{19}$ reaction. This measurement has recently been carried out in this laboratory by W. Whaling and C. Mileikowsky[36] . It is therefore of interest to see how well the predicted value agrees with the measured one.

The $F^{20}$ - $Ne^{20}$ mass difference and the $Ne^{21}(d\alpha)F^{19}$ Q-value in themselves are of importance since they provide Q-value links between the elements lighter than fluorine and those heavier than neon. Based solely upon nuclear transmutation energies, the masses of the nuclei heavier than neon can then be related to $O^{16}$. This has recently been done by C. W. Li[9] of this laboratory.

## EXPERIMENTAL METHOD

Radioactive $F^{20}$ ($T_{\frac{1}{2}}$ = 11.4 sec.) was produced by the $F^{19}(dp)F^{20}$ reaction; $CaF_2$ targets were bombarded with 2.3 Mev deuterons from the 3-Mev Kellogg Radiation Laboratory electrostatic generator. The deuteron beam was brought directly into the vacuum chamber of the spectrometer to bombard targets at the source position. The electron detector was a magnetically compensated stilbene scintillation counter (see Fig.12). Experimentally, it was observed (see Part II) that the pulse height output of the counter was directly proportional to the energy of the electrons being focused. This useful property enables one to distinguish between direct and scattered electrons, since the latter are usually much degraded in energy. One therefore has to run integral bias curves and see whether or not the integral bias steps move properly with respect to the energy of the electrons supposedly being focused. In this manner it was shown, see next section, that the counts beyond the end-point of the intense beta component are predominantly scattered electrons and room background. The monitor counter was a conventional Geiger counter which was shielded by lead (except in the direction of the target) to reduce its background counting rate.

Primarily to avoid counting the intense prompt radiation, the counters were turned off during a 6 second bombardment period. An 0.2 second delay was introduced between the end of the bombardment and the turning on of the counters to insure that only the delayed radiation was being counted and monitored. During the 5.8 second counting period, the deuteron beam was intercepted by a tantalum-backed beam chopper. This cycle was repeated until the monitor counter recorded a fixed number of gamma-ray counts, which indicated that a certain

number of beta disintegrations had occurred. The turning on and off of the counters and the operation of the beam chopper were accomplished by a system of relays actuated by a synchronous motor.

## ELECTRON SPECTRUM

For the beta spectrum measurements, a thin layer of $CaF_2$ was evaporated on 0.1 mil nickel foil. This foil was supported by a 5 mil aluminum foil which had a 3/8 inch hole in its center. The observed momentum spectrum is shown in Fig. 27. Beyond the 5.42 Mev end-point of the intense beta component, the counts do not go to zero. In order to ascertain the nature of these counts, the energy distribution of the electrons at a spectrometer setting of 5.69 Mev was analyzed by running an integral bias curve with the scintillation counter detector. To show that the counter was operating satisfactorily and also for purposes of comparison, integral bias curves were also run at spectrometer settings corresponding to 5.22, 4.74, 4.27, and 3.80 Mev. The results are shown in Fig. 28. These curves have been normalized to take account of the fact that the beta spectrum counts beyond the maximum decrease with increasing energy. The 5.22 Mev curve, being close to the end-point, has been corrected for background and for the effects of scattered electrons. Both produce a pronounced sloping plateau on the 5.22 Mev integral bias curve. The 5.69 Mev curve has only been corrected for background: an integral bias curve was taken with zero spectrometer current and then subtracted from the observed 5.69 curve*. The zero current integral bias curve is shown in Fig. 29

* To be strictly correct, the high field and not the zero current background should be subtracted. The two are the same since the background tail of Fig. 27 at high fields runs into the zero current background.

(curve with circles), and represents the energy distribution of room background and background from the $F^{20}(\beta^-)Ne^{20}$ reaction.

In Fig. 28, it is seen that the integral bias curves below the 5.69 Mev curve all show a plateau, indicating that electrons of one energy are being counted. More important, the integral bias steps move correctly with respect to the energy of the electrons being focused. The 5.69 Mev curve shows no plateau; in particular, since the integral bias curve is a sloping straight line, its differential bias curve is a rectangle, which indicates that all energies below a certain maximum are equally probable. This end-point lies roughly at 4 Mev, and this is the maximum energy of the electrons present although the spectrometer is set to focus electrons of 5.69 Mev kinetic energy. These curves show rather convincingly that the counts beyond the end-point of the intense beta component, after subtracting background, are almost entirely caused by scattered electrons.

The 5.69 Mev integral bias curve has been examined in greater detail in order to ascertain how many of the recorded counts are background and scattered electrons and how many could reasonably be attributed to a high energy component arising from a ground state beta transition. The situation is depicted in Fig. 29. The momentum spectrum of Fig. 27 was run with a counter bias of 10 volts, which corresponds to counting all electrons whose energy is greater than 900 Kev. The number of counts at 5.69 Mev was 779, and this agrees with the number observed at a setting of 10 volts on the 5.69 Mev integral bias curve. In Fig. 29 the curve with the dots corresponds to the 5.69 Mev curve with background included. The curve with the circles corresponds

to the integral bias curve of the background taken with zero spectrometer current. At 100 volts, the difference between the two curves amounts to 3 counts. These counts are presumably scattered electrons, but the possibility that they represent high energy beta-rays cannot be excluded. Since 100 volts corresponds to the setting at which a 5.69 Mev integral bias step reaches half maximum, the maximum number of high energy counts that could be present is six. This is depicted in B of Fig. 29. Therefore of the 779 counts recorded at a bias setting of 10 volts and a spectrometer setting of 5.69 Mev, 490 counts are due to background. The remaining 289 counts (0.5% of the peak of the beta spectrum) are due almost entirely to scattered electrons as shown in Fig. 28. If a high energy beta component were present, then not more than 6 of the 289 counts could reasonably be attributed to it. Beta-ray branching to the ground state of $Ne^{20}$, if present, is then estimated to have a relative intensity of less than $2.4 \times 10^{-4}$ of the main excited state transition.

Subtracting out the background and making the usual Fermi-Kurie plot yielded the straight line of Fig. 30. A straight line fits the data from the end-point on down to 400 Kev. The dashed portion represents data taken after the counter bias was reduced to count all electrons of energy $\geq 400$ Kev. A least squares analysis of the four sets of data gave an end-point energy of $5.419 \pm 0.010$ Mev*. The probable error includes the random errors as well as an estimate of the systematic errors.

---

* The quoted end-point value includes a 3 Kev correction for energy loss in the Ni foil.

## GAMMA RADIATION SPECTRUM

For the delayed gamma-ray measurements, a 40 mil $CaF_2$ crystal, 150 mil copper absorber, and a 23.2 mg/cm$^2$ thorium converter were used. The observed spectrum is shown in Fig. 31. One sees the Compton edge, K, and L photo-peaks from a single gamma-ray. No gamma-rays of energy 1 and 2.45 Mev with an intensity comparable with the main gamma transition are observed.* From the linearity of the Fermi-Kurie plot, Fig. 30, in the region around 4.60 Mev, it is concluded that if a 2.45 Mev gamma-ray were associated with the $F^{20}$ beta-decay, its intensity is less than 1 percent of the main gamma transition. Similarly, the analysis of the 5.69 Mev integral bias curve has shown the absence of beta transitions to levels below the 1.627 Mev level in $Ne^{20}$. Hence if a 1 Mev gamma-ray were associated with the $F^{20}$ beta-decay, its intensity is less than $2.4 \times 10^{-4}$ of the main gamma transition.

The gamma-ray energy was obtained by adding the K binding energy of thorium plus a converter shift correction[5] to the measured energy of the K photo-electrons. An average of four independent determinations yielded 1.627 ± 0.005 Mev as the gamma-ray energy. The position of the Compton edge is consistent with a gamma-ray of this energy. The K photo-peak is shown enlarged in the upper right hand corner of Fig.31.

Primarily to check upon the accuracy of the gamma-ray measurements, the 1.3332 ± 0.0015 Mev $Co^{60}$ photo-electric peak was run using the same absorber and converter geometry. An average of two determinations gave 1.332 Mev as the gamma-ray energy. The error lies within the

---

* Scintillation spectrometer studies on the delayed radiation confirm this result.

quoted probable error of ± 0.005 Mev for the gamma-ray measurement.

## DISCUSSION

The present investigation shows the beta and gamma spectrum of the $F^{20}$ beta-decay to be simple: the beta-decay proceeds to an excited state of $Ne^{20}$ which decays by emitting 1.627 ± 0.005 Mev gamma radiation. These results are in agreement with the results of Alburger and in disagreement with the results of Jelley and Littauer.

Adding a 1 Kev correction for recoil (calculated correction being .92 Kev), the $F^{20}$ - $Ne^{20}$ atomic mass difference is 7.047 ± 0.011 Mev. This is in agreement with the value 7.038 ± 0.018 Mev determined by Alburger[33]. Using Li's value of 20.006350 ± 17 MU for the mass of $F^{20}$[9], the $Ne^{20}$ mass is 19.998782 ± 21 MU. The conversion factor of 931.152 Mev per MU was used. This value for the $Ne^{20}$ mass is in agreement with the mass spectroscopic determinations of Ewald: 19.998771 ± 12 MU[37], and of Nier: 19.998835 ± 43 MU[38], the latter within the combined probable errors.

Using the Q-values for the $F^{19}(dp)F^{20}$ and $Ne^{20}(dp)Ne^{21}$ reactions, the predicted Q-value for the $Ne^{21}(d\,\alpha)F^{19}$ reaction is 6.442 ± 0.017 Mev. This is in agreement with the value as determined by Whaling and Mileikowsky: 6.432 ± 0.010 Mev[36].

The end-point energy of 5.419 ± 0.010 Mev coupled with a half-life of 11.4 seconds gives an ft-value of $9.73 \times 10^4$ seconds for the excited state transition. This value is considerably higher than the ft-values for the class of mirror nuclei transitions, ft between 1000-5000 seconds. The transition is allowed unfavored in the sense that the wave functions for the final and initial nucleon states do not quite overlap.

The transition is $\Delta J = 0, 1$; no. Since the parity of the $F^{20}$ ground state is even[39], the first excited state in $Ne^{20}$ must then also have even parity. This is not in agreement with the results of Huby and Newns[40]; they find that the 1.63 Mev level in $Ne^{20}$ has odd parity.

Using the upper limit of $2.4 \times 10^{-4}$ for the ground state branching ratio, the minimum ft-value for the ground state transition is $1.3 \times 10^{9}$ seconds ($\log ft \geq 9.1$). According to Nordheim's[41] empirical classification of ground state beta transitions involving even A nuclei, this transition is at least first forbidden ($\Delta J = 2$; Yes). An $\ell$-forbidden transition ($\Delta J = 1$; No, $\Delta \ell = 2$) is just possible since the log ft-values for this class of transitions range between 5.0 to 9.0. The remaining alternative is that the transition is second or higher forbidden ($\Delta J = 2$; No, or $\Delta J > 2$). Since the $F^{20}$ ground state has even parity[39], the only alternatives possible are the $\ell$, second, and higher forbidden transitions as the $Ne^{20}$ ground state is presumably even parity. Since the $Ne^{20}$ ground state is presumably spin zero, the possible assignments for the $F^{20}$ ground state are then 1+, 2+, and 3+, the 1+ being barely possible.

The recently published results of Bromley, et al.[39], indicate that the ground state of $F^{20}$ is 1+. The ground state transition is then $\Delta J = 1$; no, and hence allowed on Nordheim's classification[41]. To explain the lack of beta transitions to the ground state as observed by Littauer[32], they postulated an $\ell$-forbidden transition as is done in the previous paragraph. They conclude that a single-particle model is inadequate to account for their observations on the $F^{20}$ ground state.

A 2+ or 3+ assignment, however, is very probable on the basis of the present experimental results. These assignments are compatible with the shell model picture: the odd proton is $s_{1/2}$ while the odd neutron is $d_{5/2}$ or $D_{3/2}$. These can combine to give 2+ or 3+.

## SUMMARY

The electron and gamma-ray spectrum associated with the $F^{20}$ beta-decay has been investigated with a magnetic lens spectrometer. The electron spectrum consists of one component of maximum energy 5.419 $\pm$ 0.010 Mev. The beta-decay proceeds to an excited state of $Ne^{20}$ which decays by the emission of 1.627 $\pm$ 0.005 Mev delayed gamma radiation. The beta spectrum is of the allowed shape: the Fermi-Kurie plot is linear from the end-point down to 400 kev. The ft-value of the transition to the excited state is $9.73 \times 10^4$ seconds.

A magnetically compensated stilbene scintillation counter has been employed to show that the counts beyond the end-point of the intense beta component are predominantly scattered electrons and room background. Beta-ray branching to the ground state of $Ne^{20}$, if present, is estimated to have a relative intensity of less than $2.4 \times 10^{-4}$ of the main excited state transition. The minimum ft-value of the transition to the ground state is then $1.3 \times 10^9$ seconds (log ft $\geq$ 9.1). This lower limit for the log ft-value suggests that the spin of the $F^{20}$ ground state could be either one, two, or three if even parity is assumed. The 1+ assignment, recently reported by Bromley et al., is just barely possible on the basis of the present experimental results.

The possible assignments for the $Ne^{20}$ excited state are 1+, 2+, and 3+ since the excited state transition is $\Delta J = 0, 1$; no. According

to the empirical rule of Goldhaber and Sunyar[42] regarding the first excited state of even-even nuclei, the assignment is most likely $2^+$.

REFERENCES


| | | |
|---|---|---|
| 1. | J. I. Hopkins, | Rev. Sci. Inst. 22, 29 (1951). |
| 2. | W. J. Ramler and M. S. Freedman, | Rev. Sci. Inst. 21, 784 (1950). |
| 3. | Jentschke et al., | Phys. Rev. 83, 170 (1951). |
| 4. | C. D. Ellis, | Proc. Roy. Soc. London A 138, 318 (1932). |
| 5. | Hornyak, Lauritsen, and Rasmussen, | Phys. Rev. 76, 731 (1949). |
| 6. | W. L. Brown, | Phys. Rev. 83, 271 (1951). |
| 7. | G. Lindström, | Phys. Rev. 83, 465 (1951). |
| 8. | Macklin, Lidofsky, and Wu, | Phys. Rev. 78, 318 (1950). |
| 9. | C. W. Li, | Phys. Rev. 88, 1038 (1952). |
| 10. | Jensen, Nichols, Clement, and Pohm, | Phys. Rev. 85, 112 (1952). |
| 11. | W. F. Hornyak and T. Lauritsen, | Phys. Rev. 77, 160 (1950). |
| 12. | B. T. Wright, | Phys. Rev. 90, 159 (1953). |
| 13. | A. K. Solomon, | Phys. Rev. 60, 279 (1941) |
| 14 | A. A. Townsend, | Proc. Roy. Soc. 177, 357 (1940, 41). |
| 15. | Siegbahn and Bohr, | Arkiv. f. Ast. Math. Fys. 30B, No. 3 (1944). |
| 16. | Siegbahn and Peterson, | Arkiv. f. Ast. Math. Fys. 32B, No. 5 (1945). |
| 17. | H. T. Richards and R. V. Smith, | Phys. Rev. 77, 752 (1950). |
| 18. | T. W. Bonner and J. W. Butler, | Phys. Rev. 83, 1091 (1951) |
| 19. | F. Ajzenberg and T. Lauritsen, | Rev. Mod. Phys. 24, 321 (1952). |

| | | |
|---|---|---|
| 20. | H. W. Newson, | Phys. Rev. 48, 790 (1935). |
| 21. | Kurie, Richardson, and Paxton, | Phys. Rev. 49, 368 (1936). |
| 22. | Bethe, Hoyle, and Peierls, | Nature 143, 200 (1939). |
| 23. | V. Perez-Mendez and P. Lindenfeld, | Phys. Rev. 80, 1097 (1950). |
| 24. | V. Perez-Mendez and P. Lindenfeld, | Phys. Rev. 83, 864 (1951). |
| 25. | R. G. Thomas and T. Lauritsen, | Phys. Rev. 88, 969 (1952). |
| 26. | W. E. Meyerhof, | Priv. Comm. to F. Ajzenberg and T. Lauritsen. |
| 27. | Roderick, Lönsjö, and Meyerhof, | Phys. Soc. Bulletin 42 (Jan 1953). |
| 28. | White, Creutz, Delsasso, and Wilson, | Phys. Rev. 59, 63 (1941). |
| 29. | Mandeville, Swann, Chatterjee, and Van Patter, | Phys. Rev. 85, 193 (1952). |
| 30. | Mayer, Moszkowski, and Nordheim, | Rev. Mod. Phys. 23, 315 (1951). |
| 31. | J. V. Jelley, | Phil. Mag. 41, 1199 (1950). |
| 32. | R. M. Littauer, | Phil. Mag. 41, 1214 (1950). |
| 33. | D. E. Alburger, | Phys. Rev. 88, 1257 (1952). |
| 34. | Van Patter, Sperduto, Endt, Buechner, and Enge, | Phys. Rev. 85, 142 (1952). |
| 35. | H. A. Watson and W. W. Buechner, | Phys. Rev. 88, 1324 (1952). |
| 36. | C. Mileikowsky and W. Whaling, | Phys. Rev. 88, 1254 (1952). |
| 37. | H. Ewald, | Zeit. F. Naturforschung, 6A, 293 (1951). |
| 38. | A. O. Nier, | Phys. Rev. 81, 624 (1951). |

| | | |
|---|---|---|
| 39. | Bromley, Bruner, and Fulbright, | Phys. Rev. 89, 396 (1953). |
| 40. | R. Huby and H. C. Newns, | Phil. Mag. 42, 1442 (1951). |
| 41. | L. W. Nordheim, | Rev. Mod. Phys. 23, 322 (1951). |
| 42. | M. Goldhaber and A. W. Sunyar, | Phys. Rev. 83, 906 (1951). |

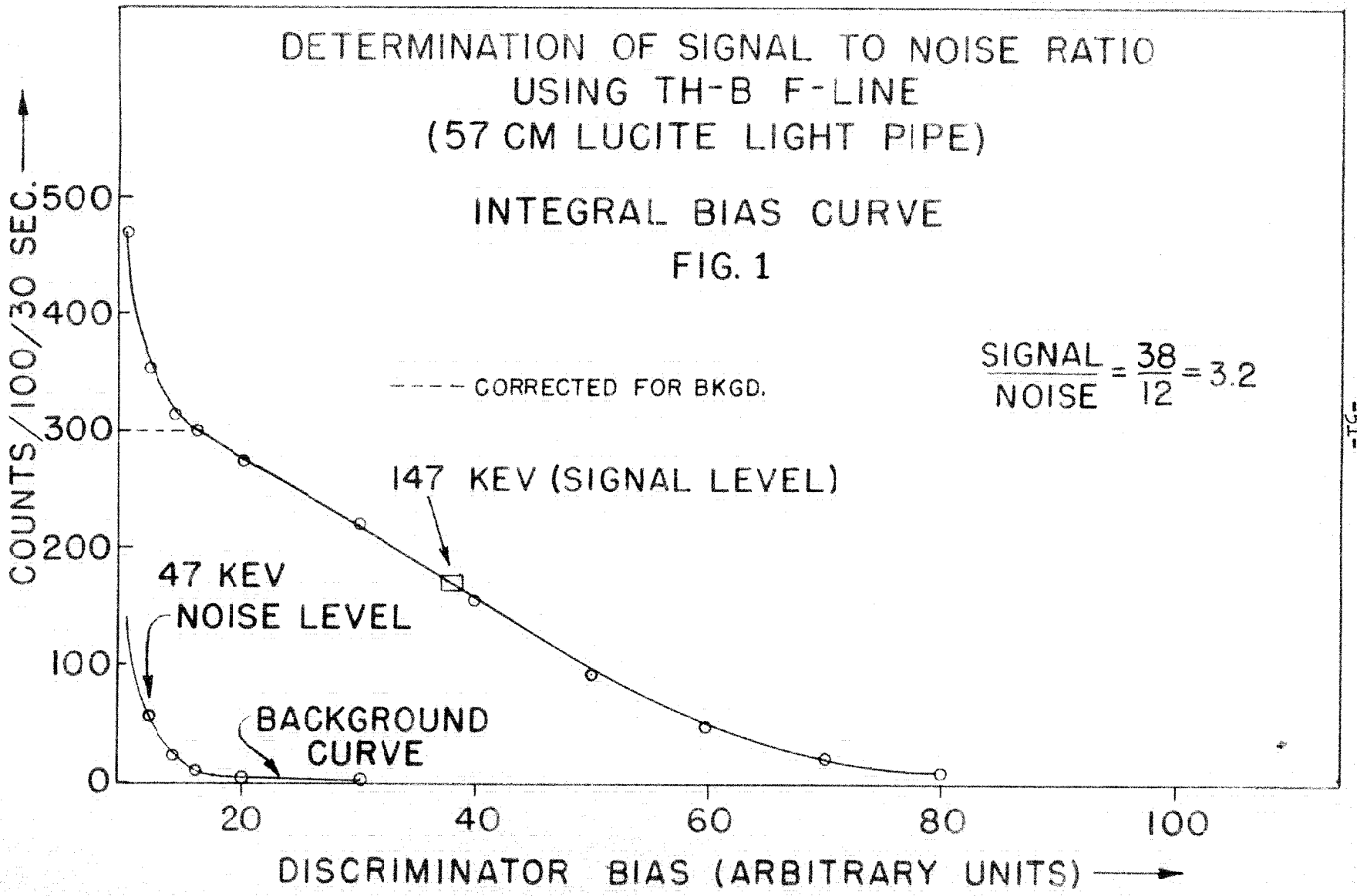
DETERMINATION OF SIGNAL TO NOISE RATIO
USING TH-B F-LINE
(57 CM LUCITE LIGHT PIPE)
INTEGRAL BIAS CURVE
FIG. 1
COUNTS/100/30 SEC.
500
400
300
200
100
0
---- CORRECTED FOR BKGD.
SIGNAL/NOISE = 38/12 = 3.2
147 KEV (SIGNAL LEVEL)
47 KEV
NOISE LEVEL
BACKGROUND
CURVE
20
40
60
80
100
DISCRIMINATOR BIAS (ARBITRARY UNITS)

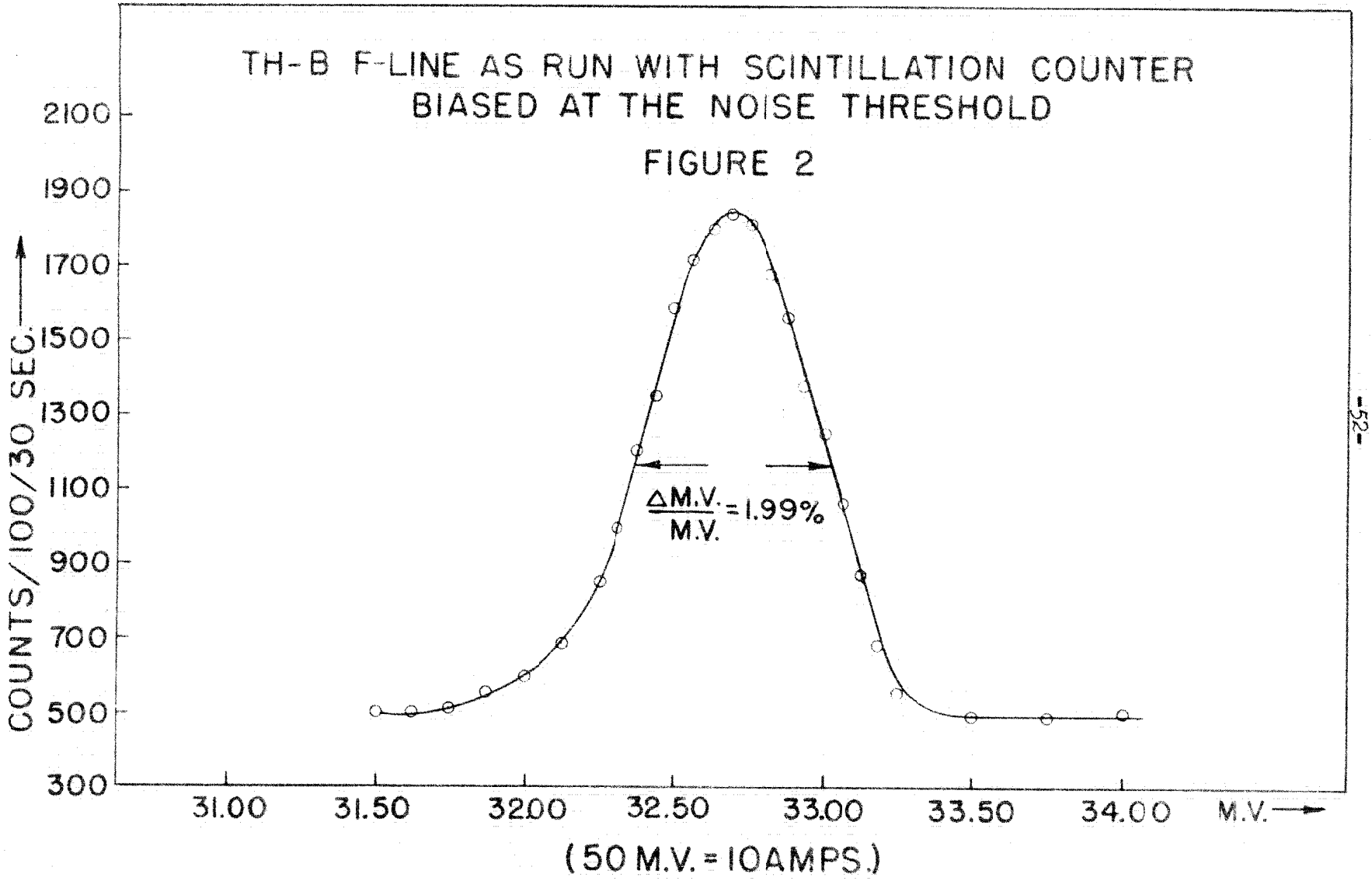
TH-B F-LINE AS RUN WITH SCINTILLATION COUNTER
BIASED AT THE NOISE THRESHOLD
FIGURE 2
COUNTS/100/30 SEC.
2100
1900
1700
1500
1300
1100
900
700
500
300
ΔM.V./M.V. = 1.99%
31.00
31.50
32.00
32.50
33.00
33.50
34.00
M.V.
(50 M.V. = 10 AMPS.)

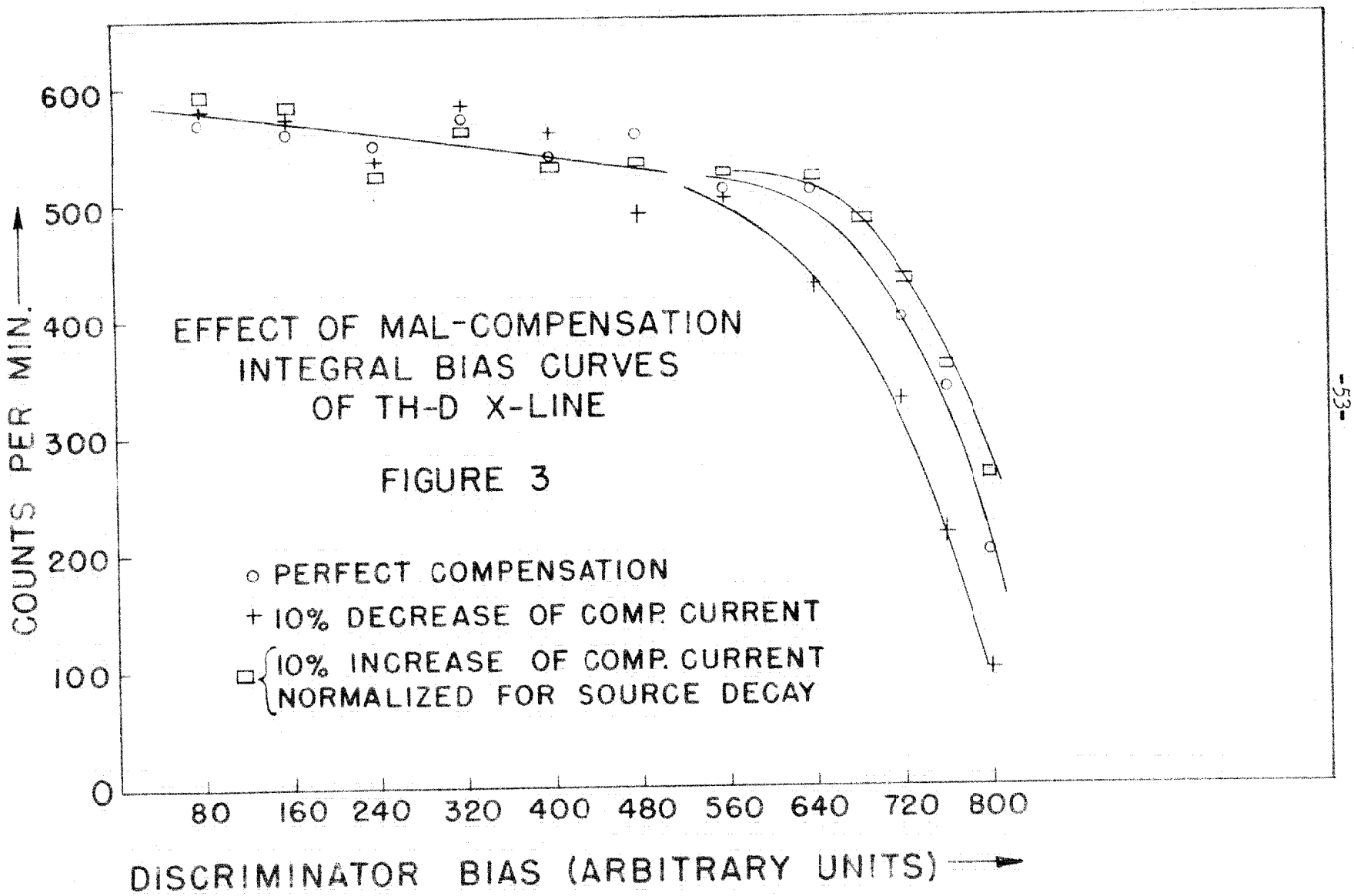
600
500
400
300
200
100
0
COUNTS PER MIN.
80
160
240
320
400
480
560
640
720
800
DISCRIMINATOR BIAS (ARBITRARY UNITS)
EFFECT OF MAL-COMPENSATION
INTEGRAL BIAS CURVES
OF TH-D X-LINE
FIGURE 3
○ PERFECT COMPENSATION
+ 10% DECREASE OF COMP. CURRENT
□ 10% INCREASE OF COMP. CURRENT
NORMALIZED FOR SOURCE DECAY

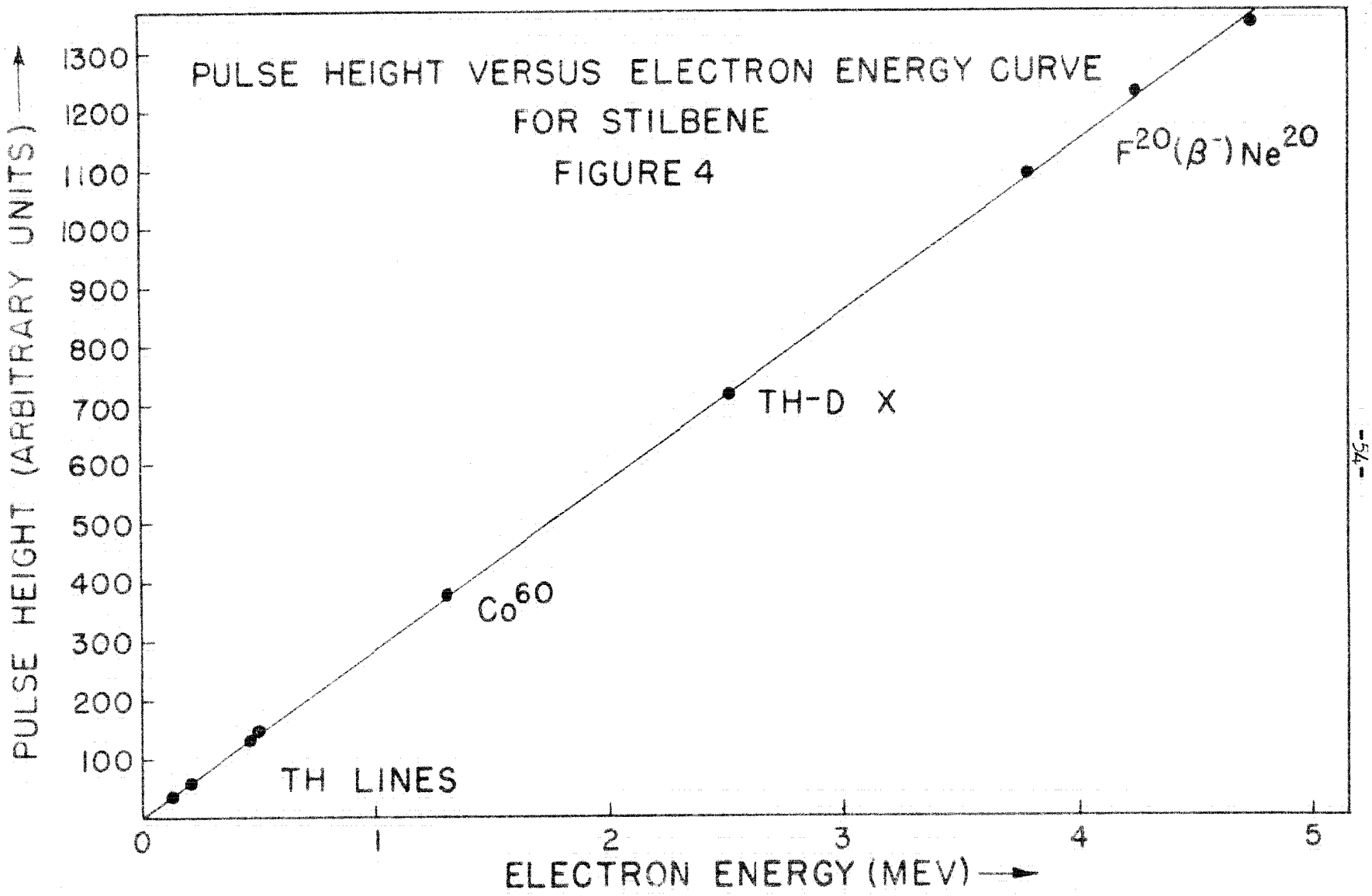
PULSE HEIGHT VERSUS ELECTRON ENERGY CURVE
FOR STILBENE
FIGURE 4
PULSE HEIGHT (ARBITRARY UNITS) →
1300
1200
1100
1000
900
800
700
600
500
400
300
200
100
TH LINES
Co60
TH-D X
F20(β⁻)Ne20
0
1
2
3
4
5
ELECTRON ENERGY (MEV) →

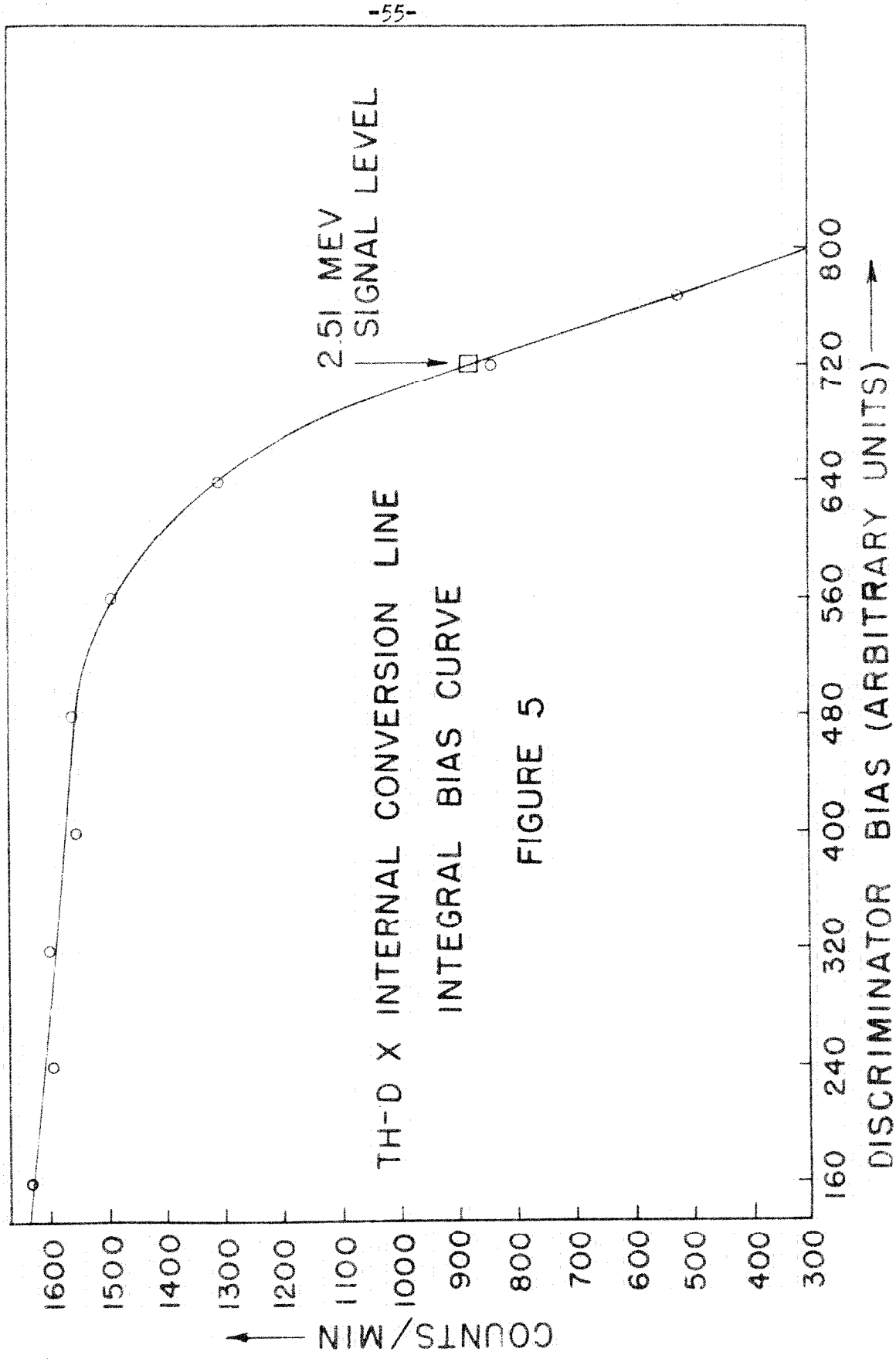
2.51 MEV
SIGNAL LEVEL
TH-D X INTERNAL CONVERSION LINE
INTEGRAL BIAS CURVE
COUNTS/MIN
DISCRIMINATOR BIAS (ARBITRARY UNITS)
1600
1500
1400
1300
1200
1100
1000
900
800
700
600
500
400
300
160
240
320
400
480
560
640
720
800

FIGURE 5

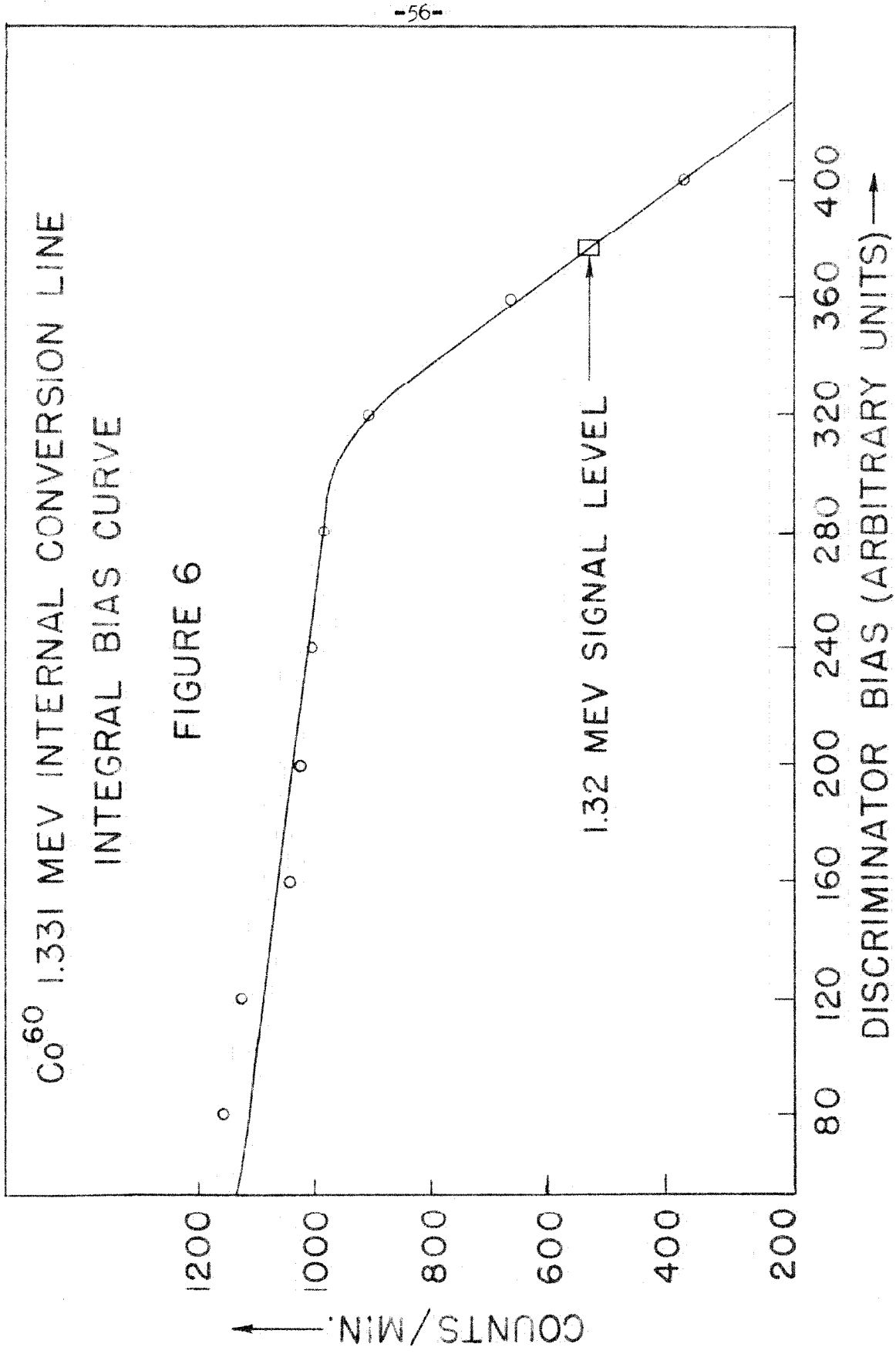
$Co^{60}$ 1.331 MEV INTERNAL CONVERSION LINE
INTEGRAL BIAS CURVE
1.32 MEV SIGNAL LEVEL
COUNTS/MIN. ←
1200
1000
800
600
400
200
80
120
160
200
240
280
320
360
400
DISCRIMINATOR BIAS (ARBITRARY UNITS) →

FIGURE 6

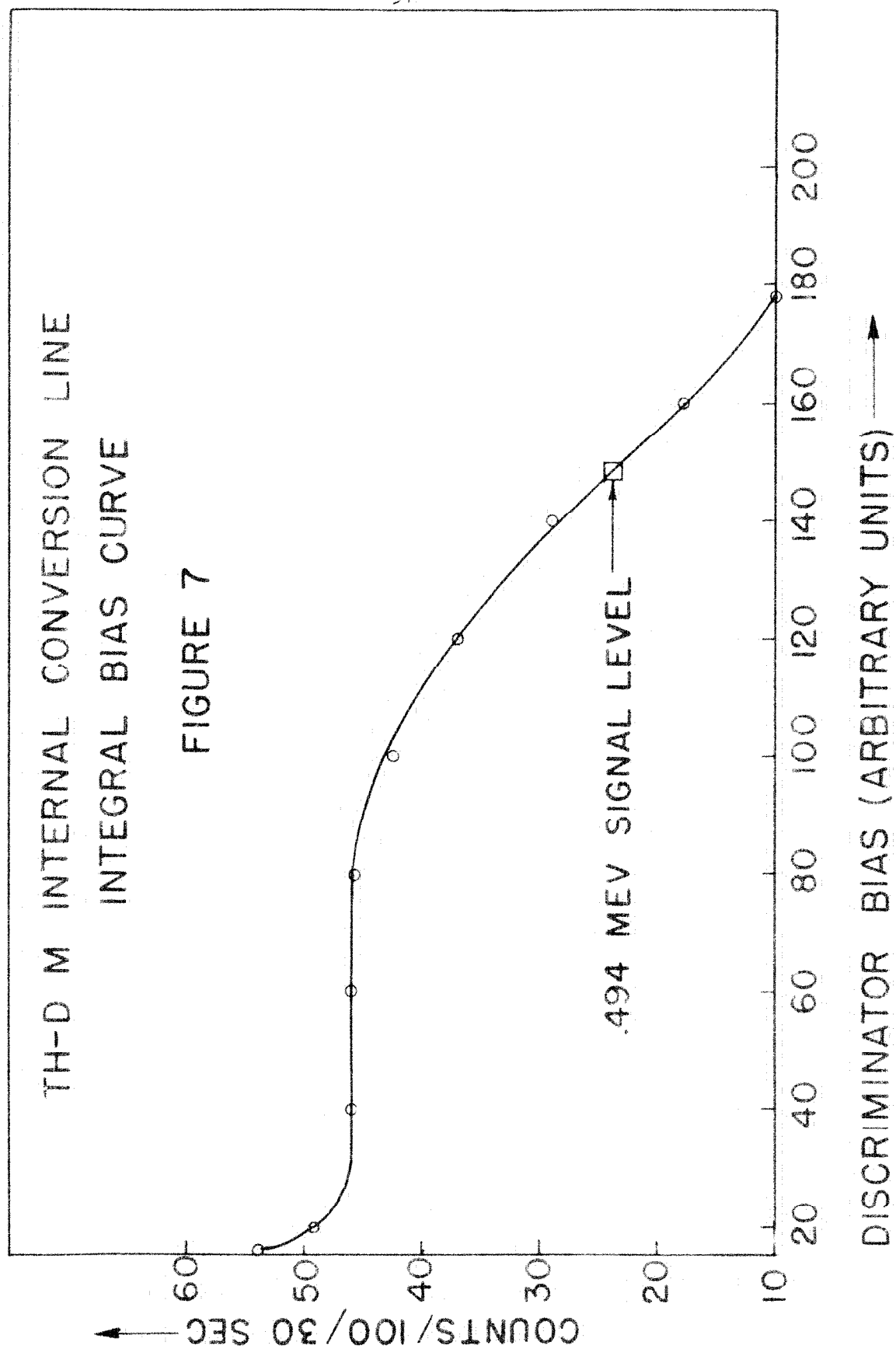
TH-D M INTERNAL CONVERSION LINE
INTEGRAL BIAS CURVE
.494 MEV SIGNAL LEVEL
COUNTS/100/30 SEC
DISCRIMINATOR BIAS (ARBITRARY UNITS)
10
20
30
40
50
60
20
40
60
80
100
120
140
160
180
200

FIGURE 7

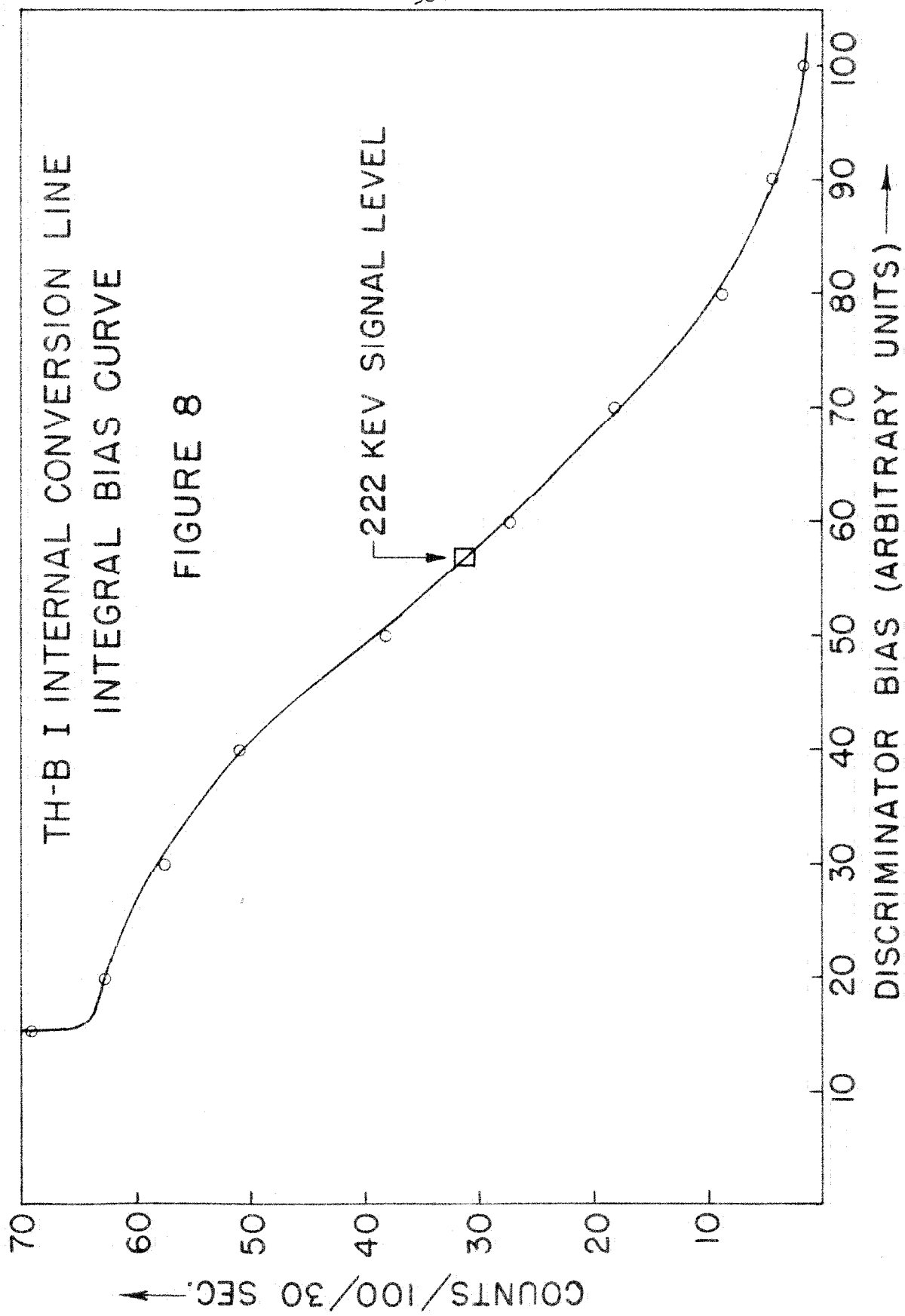
TH-B I INTERNAL CONVERSION LINE
INTEGRAL BIAS CURVE
222 KEV SIGNAL LEVEL
COUNTS/100/30 SEC.
DISCRIMINATOR BIAS (ARBITRARY UNITS)
10
20
30
40
50
60
70
80
90
100

FIGURE 8

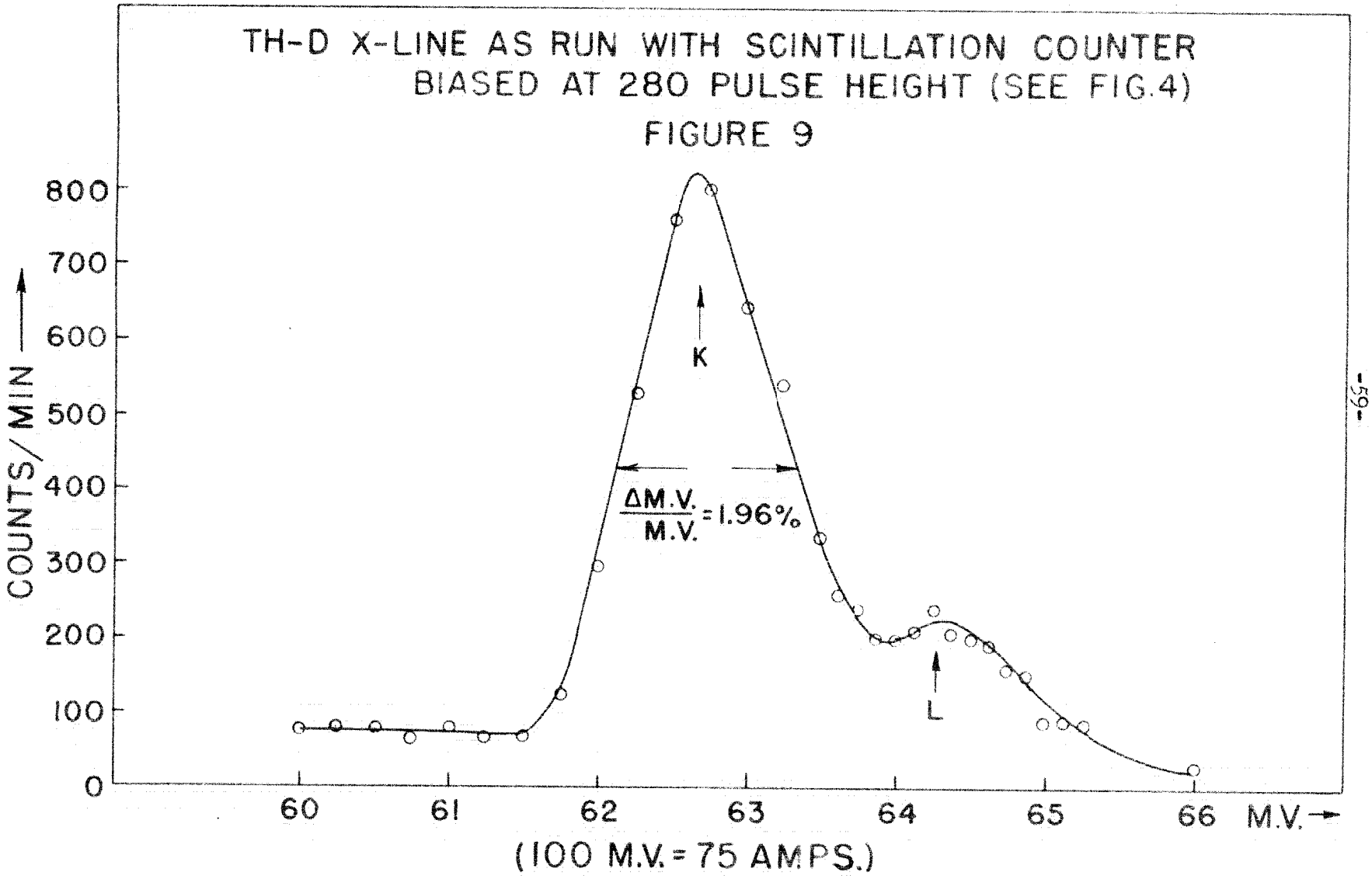
TH-D X-LINE AS RUN WITH SCINTILLATION COUNTER
BIASED AT 280 PULSE HEIGHT (SEE FIG.4)
FIGURE 9
COUNTS/MIN
800
700
600
500
400
300
200
100
0
K
L
ΔM.V./M.V. = 1.96%
60
61
62
63
64
65
66
M.V.
(100 M.V. = 75 AMPS.)

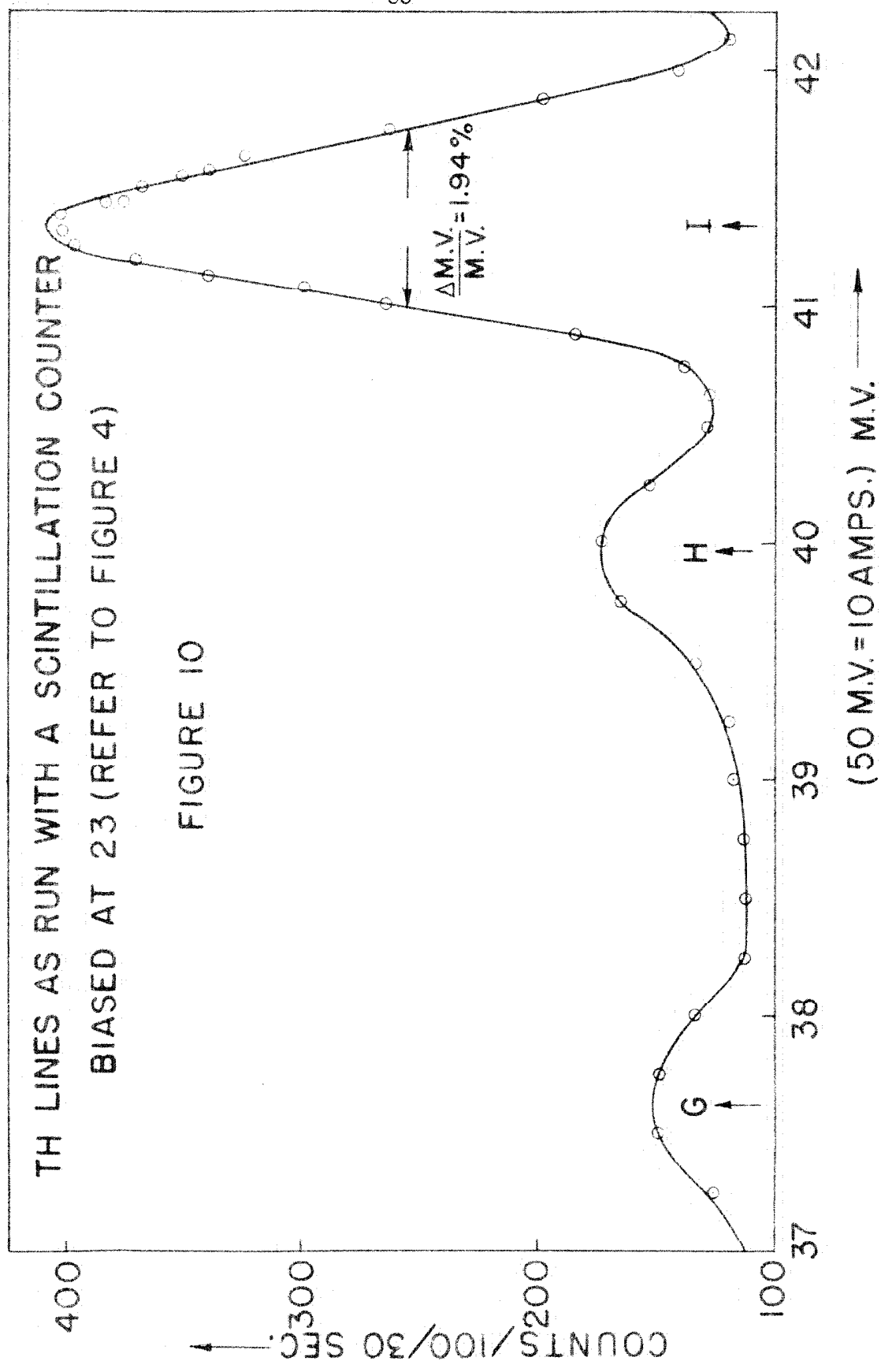
TH LINES AS RUN WITH A SCINTILLATION COUNTER
BIASED AT 23 (REFER TO FIGURE 4)
ΔM.V./M.V. = 1.94%
G
H
I
COUNTS/100/30 SEC.
400
300
200
100
37
38
39
40
41
42
(50 M.V. = 10 AMPS.) M.V.

FIGURE 10

FIGURE 11

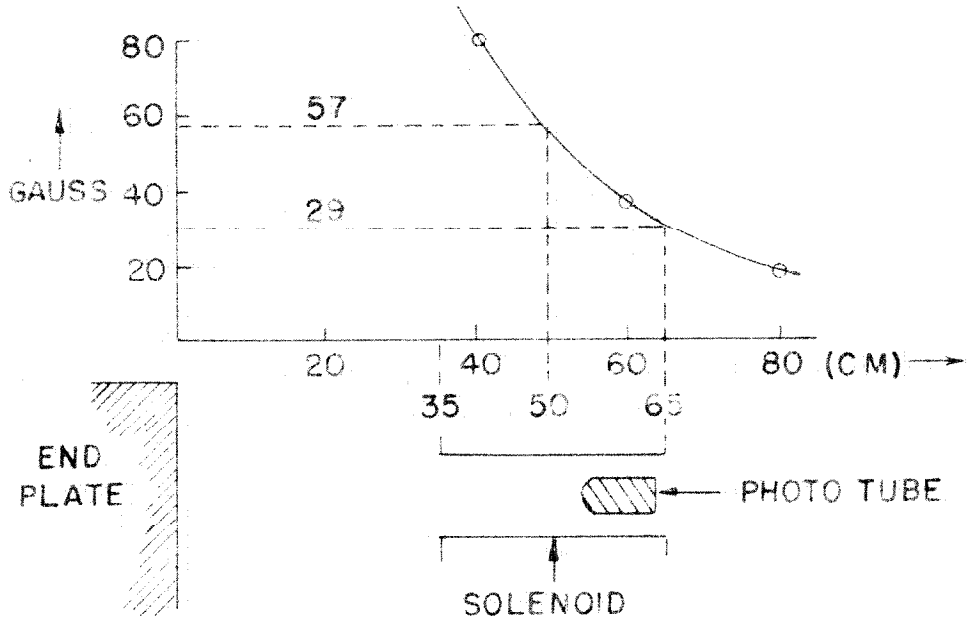


FIELD MEASUREMENTS ARE FOR A SPECTROMETER CURRENT OF 38 AMPERES

FIGURE 12

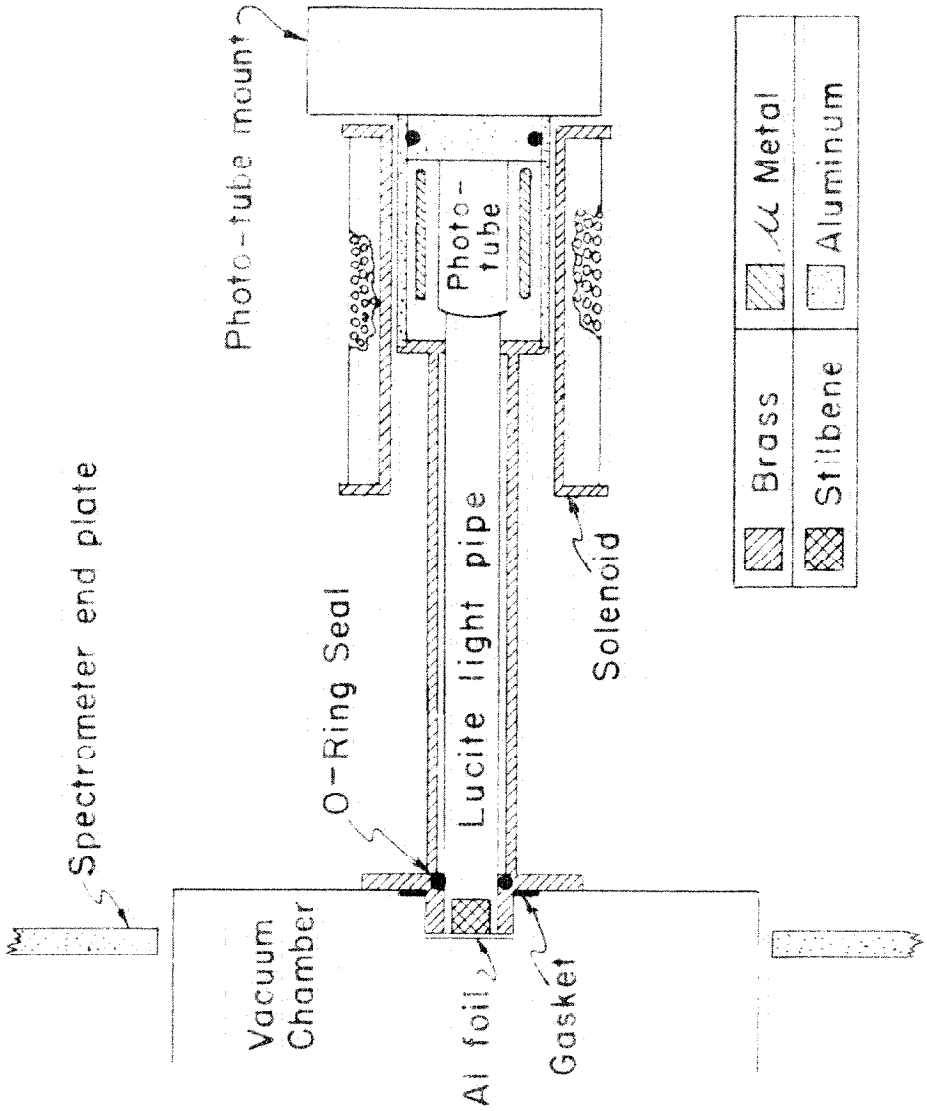
Photo-tube mount
Photo-tube
Spectrometer end plate
O-Ring Seal
Lucite light pipe
Solenoid
Vacuum Chamber
Al foil
Gasket
Brass
μ Metal
Stilbene
Aluminum

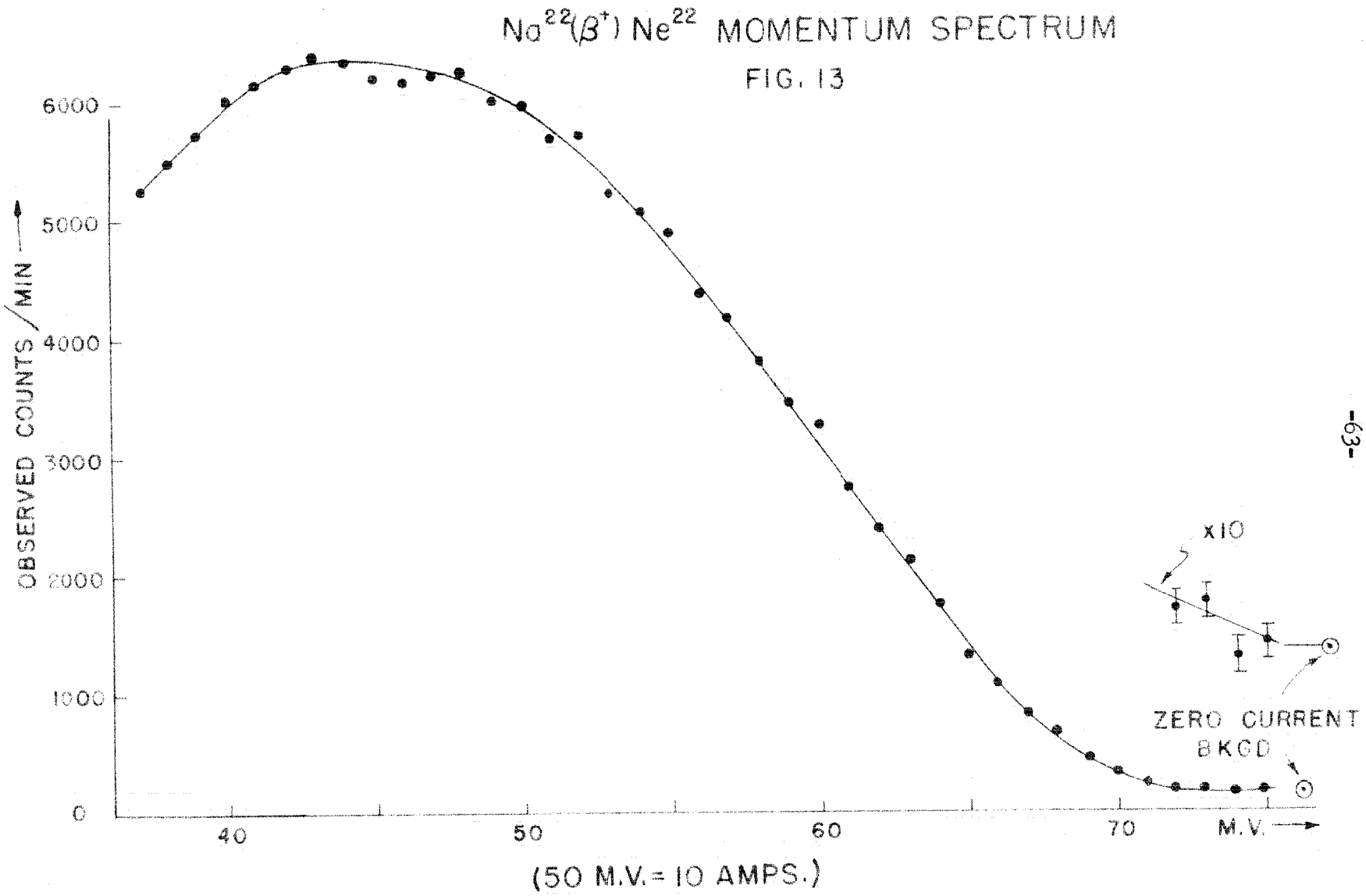
$Na^{22}(\beta^+)\,Ne^{22}$ MOMENTUM SPECTRUM
FIG. 13
OBSERVED COUNTS / MIN
6000
5000
4000
3000
2000
1000
0
40
50
60
70
M.V.
x10
ZERO CURRENT
BKGD
(50 M.V. = 10 AMPS.)

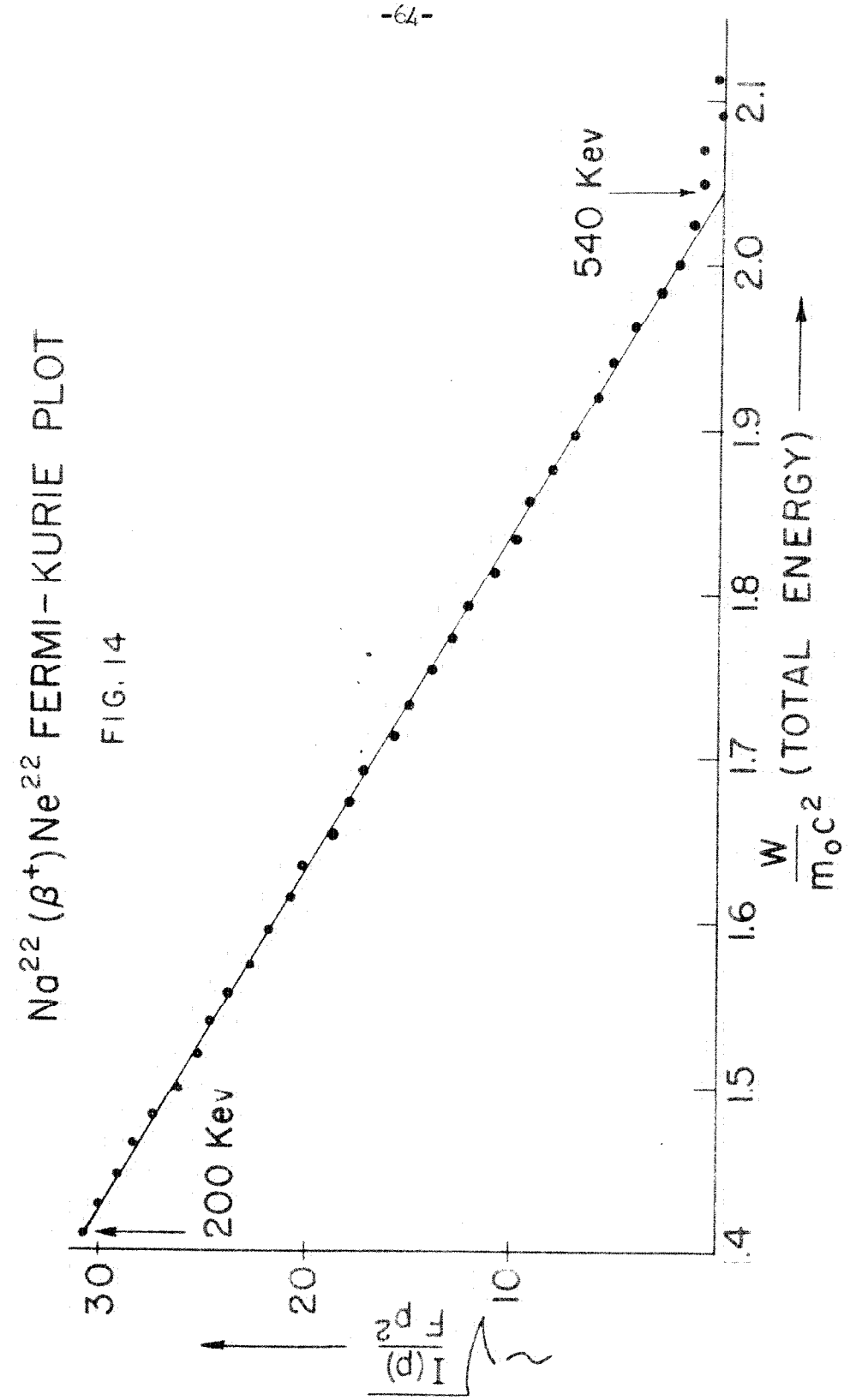
$Na^{22}(\beta^+)Ne^{22}$ FERMI-KURIE PLOT
FIG. 14
$\sqrt{\frac{I(p)}{\pi p^2}}$
30
20
10
200 Kev
540 Kev
.4
1.5
1.6
1.7
1.8
1.9
2.0
2.1
$\frac{W}{m_o c^2}$ (TOTAL ENERGY)

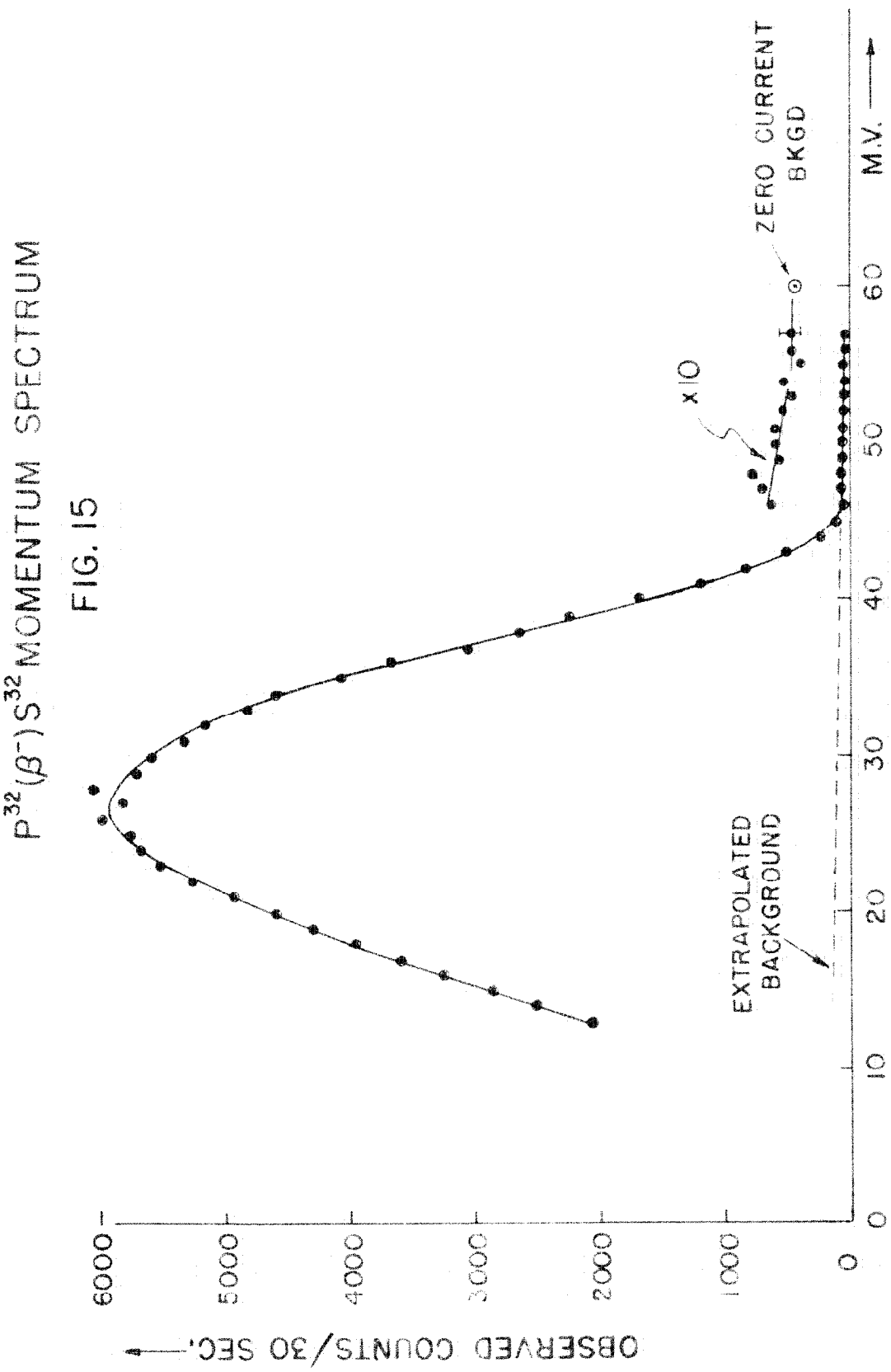
P32(β−)S32 MOMENTUM SPECTRUM
FIG. 15
OBSERVED COUNTS/30 SEC.
6000
5000
4000
3000
2000
1000
0
10
20
30
40
50
60
M.V.
(100 M.V.= 75 AMPS.)
EXTRAPOLATED BACKGROUND
x10
ZERO CURRENT BKGD

$P^{32}(\beta^-)S^{32}$ FERMI-KURIE PLOT

FIGURE 16

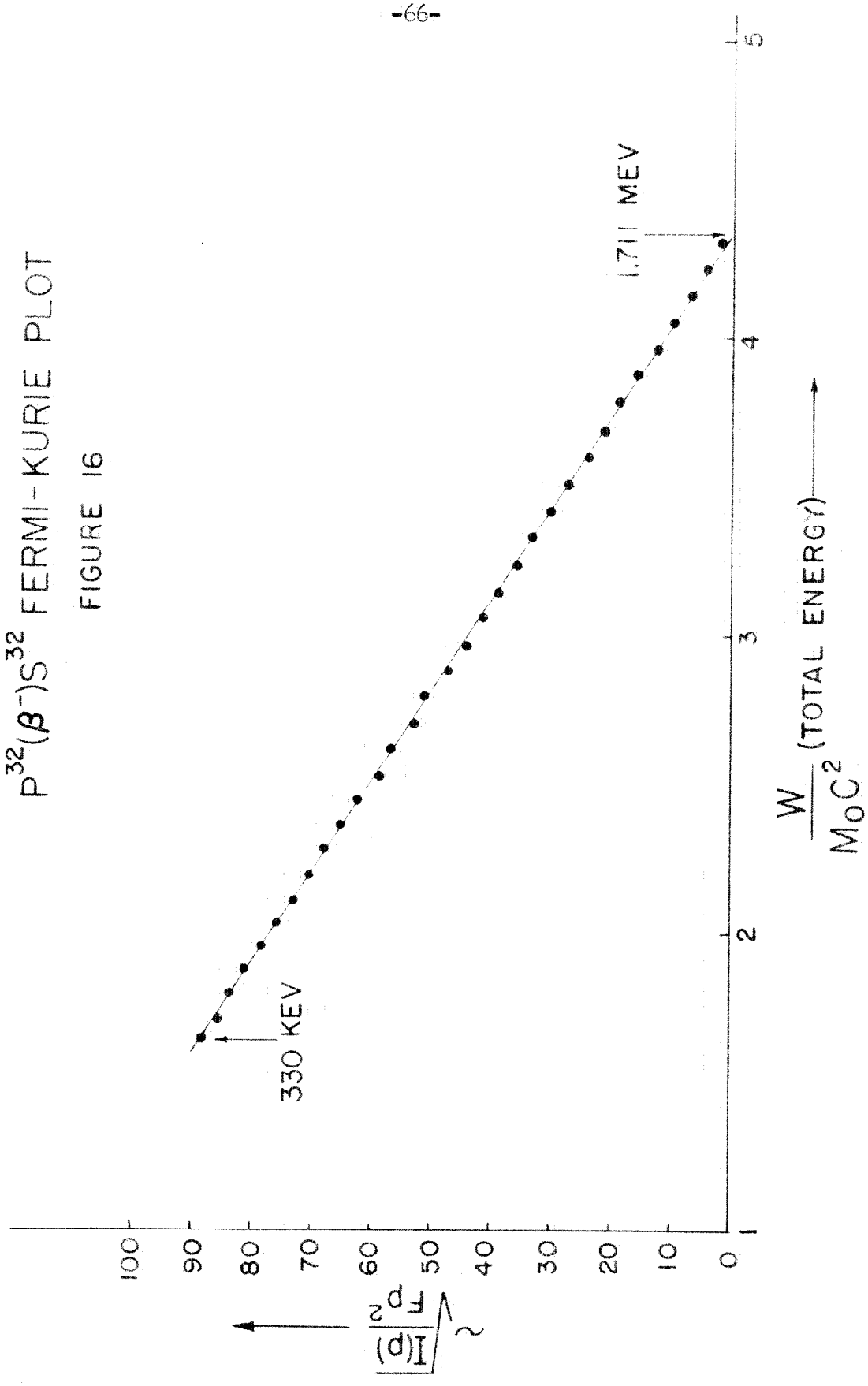

INTEGRAL BIAS CURVES OF THE $P^{32}$ BETA SPECTRUM

FIG. 17

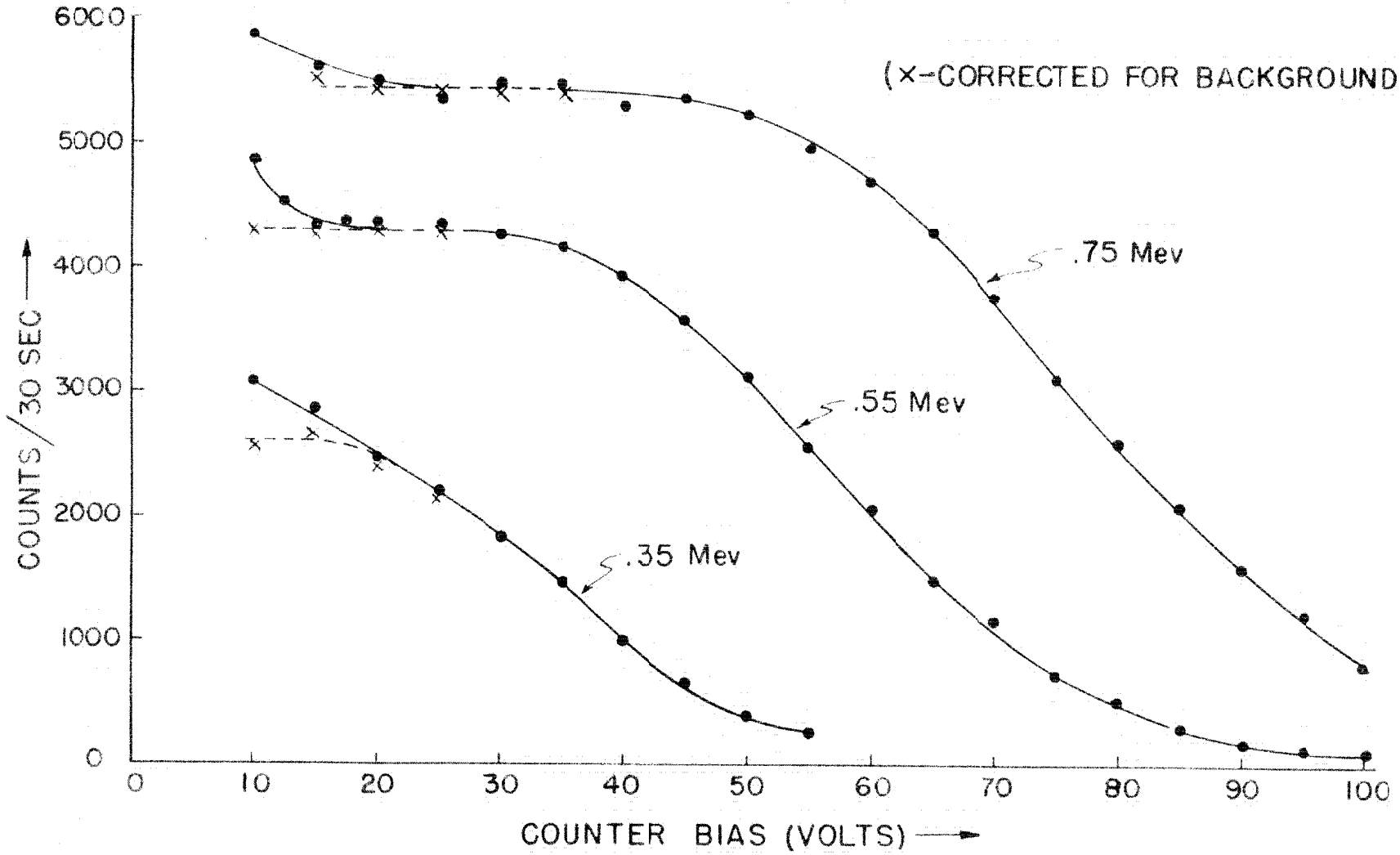

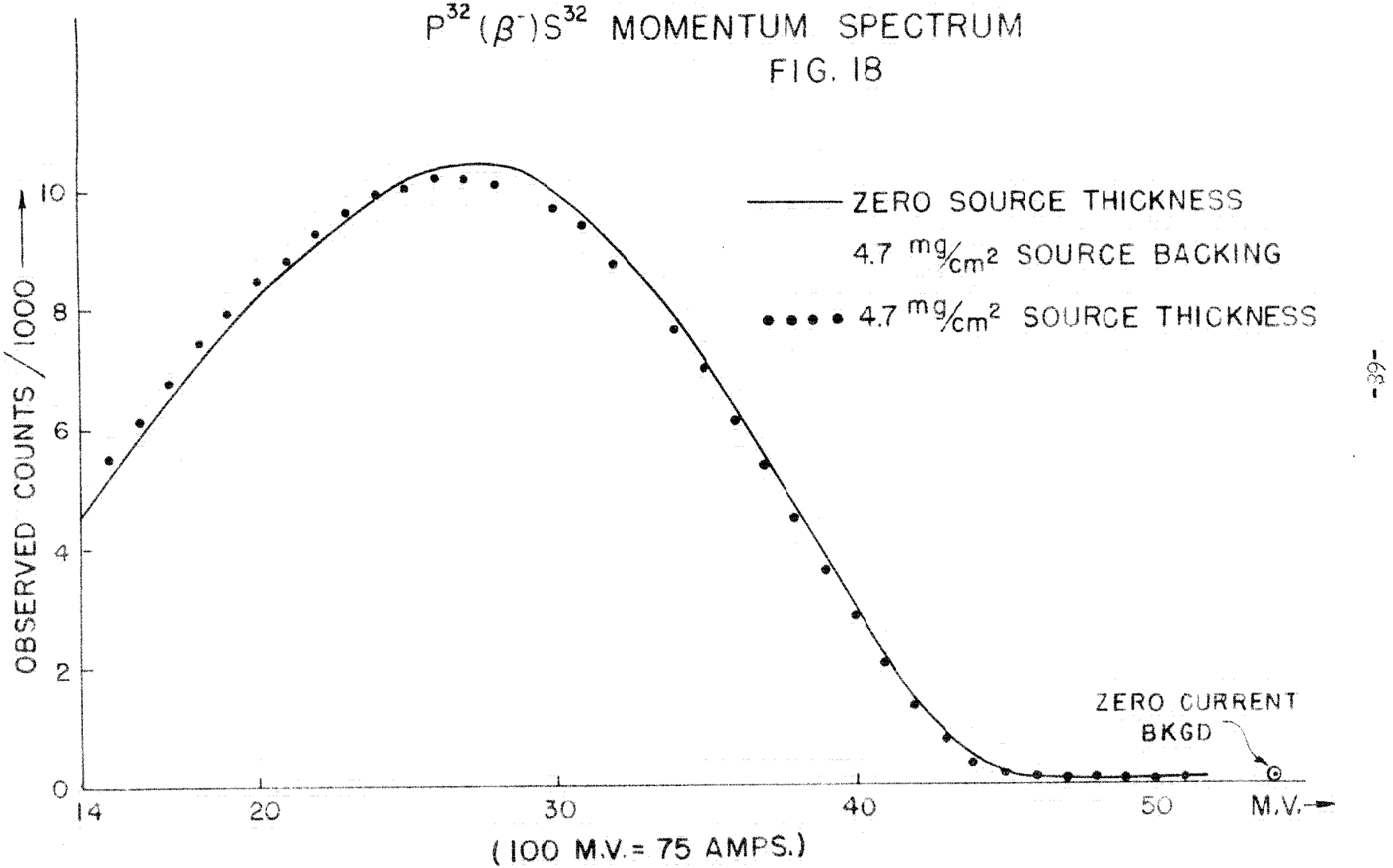
P32 (β-) S32 MOMENTUM SPECTRUM
FIG. 18
ZERO SOURCE THICKNESS
4.7 mg/cm2 SOURCE BACKING
4.7 mg/cm2 SOURCE THICKNESS
OBSERVED COUNTS / 1000
0
2
4
6
8
10
14
20
30
40
50
M.V.
ZERO CURRENT BKGD
(100 M.V. = 75 AMPS.)

$P^{32}(\beta^-)S^{32}$ FERMI-KURIE PLOT

FIG. 19

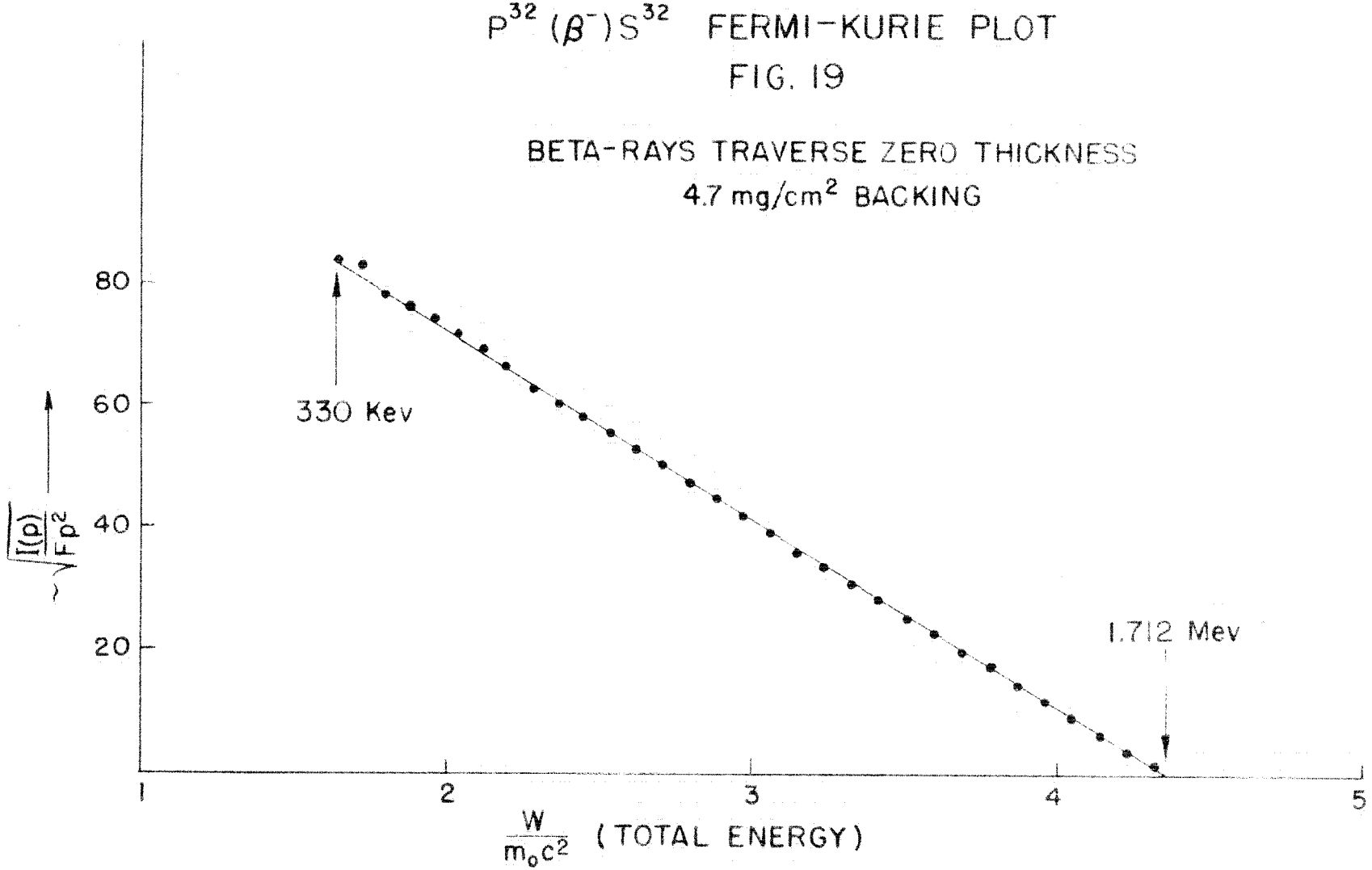

# $P^{32}(\beta^-)S^{32}$ FERMI-KURIE PLOT

FIG. 20

BETA-RAYS TRAVERSE 4.7 mg/cm$^2$ OF QUARTZ

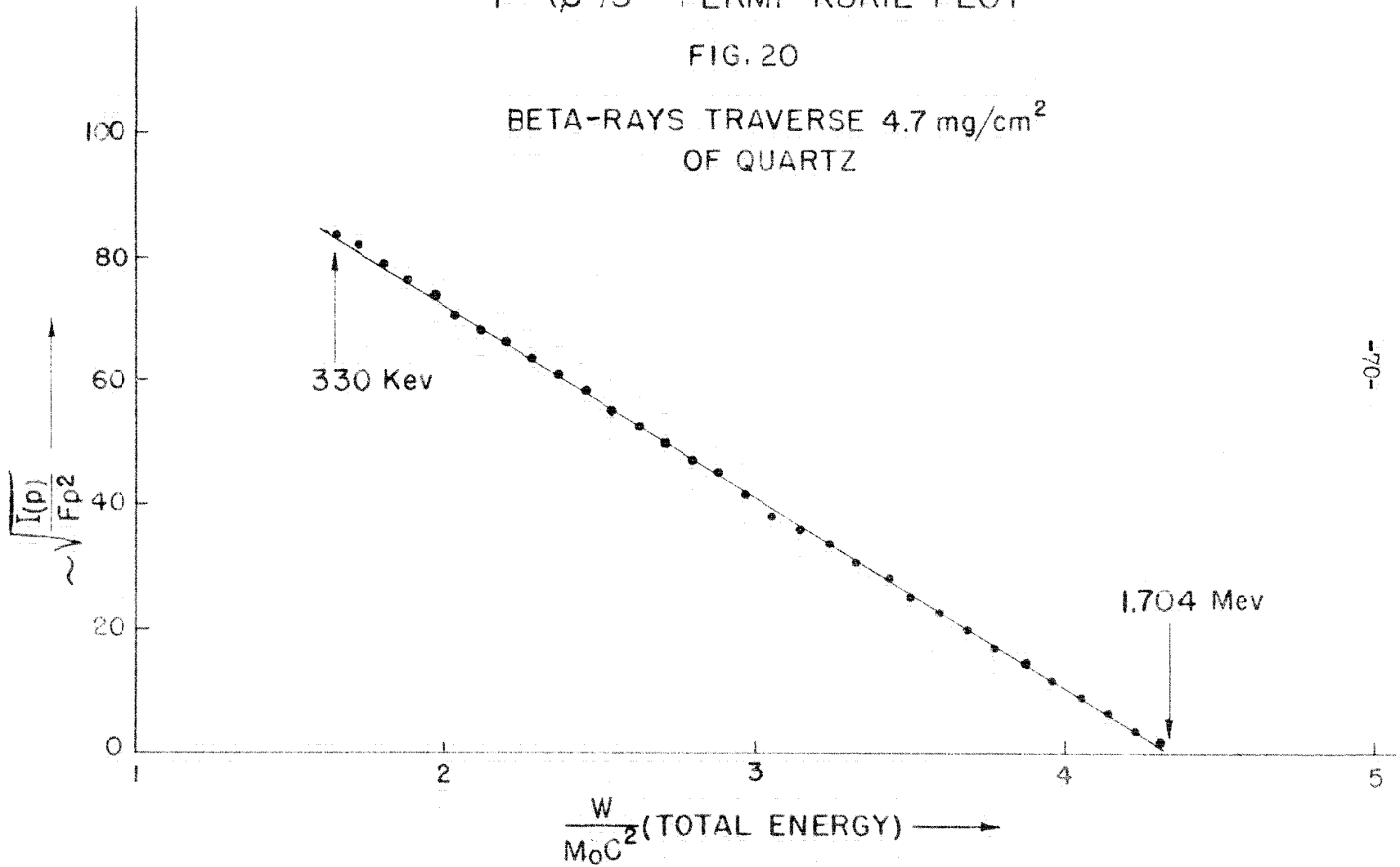

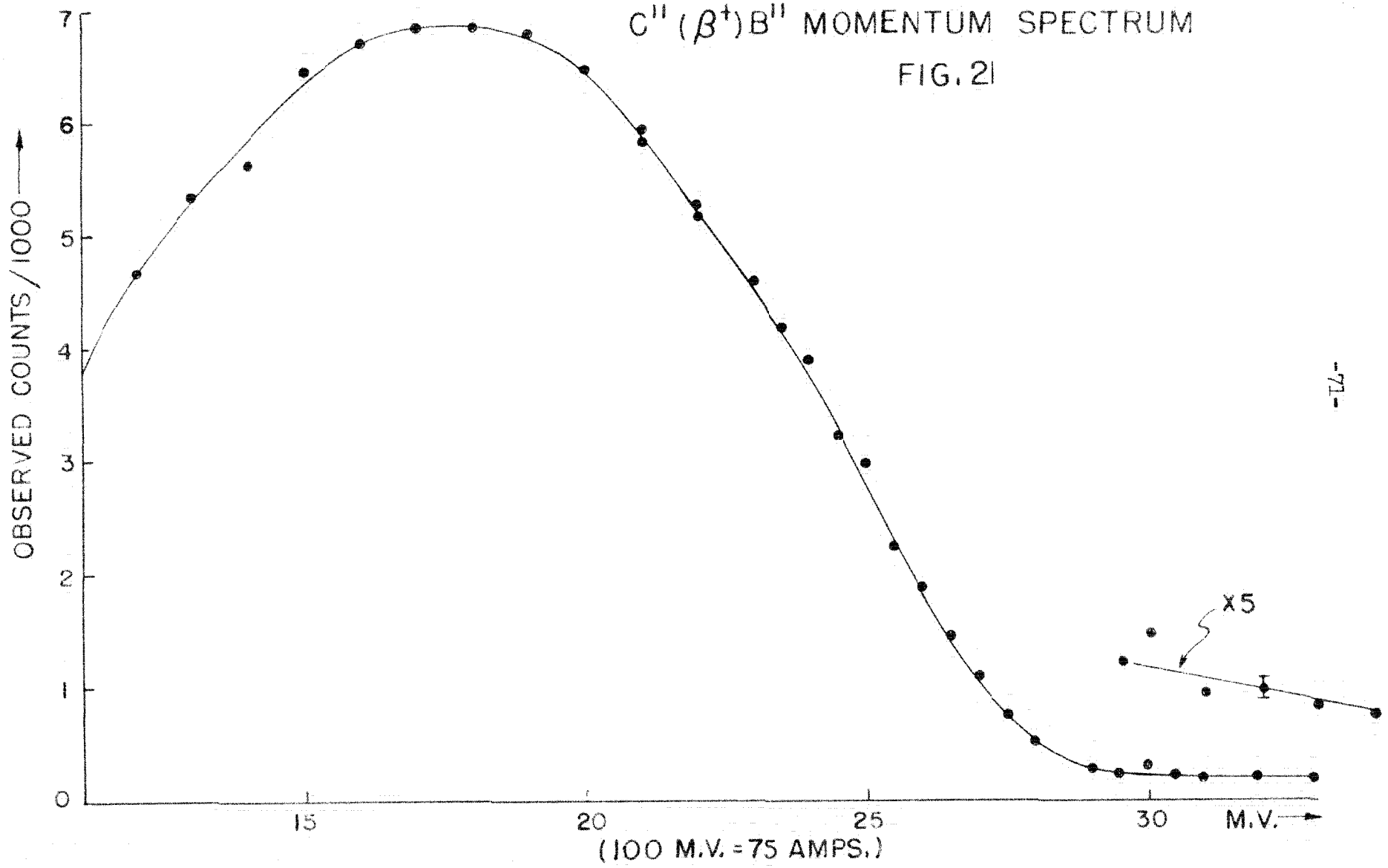
C11 (β+) B11 MOMENTUM SPECTRUM
FIG. 21
OBSERVED COUNTS / 1000
0
1
2
3
4
5
6
7
15
20
25
30
M.V.
(100 M.V. = 75 AMPS.)
X5

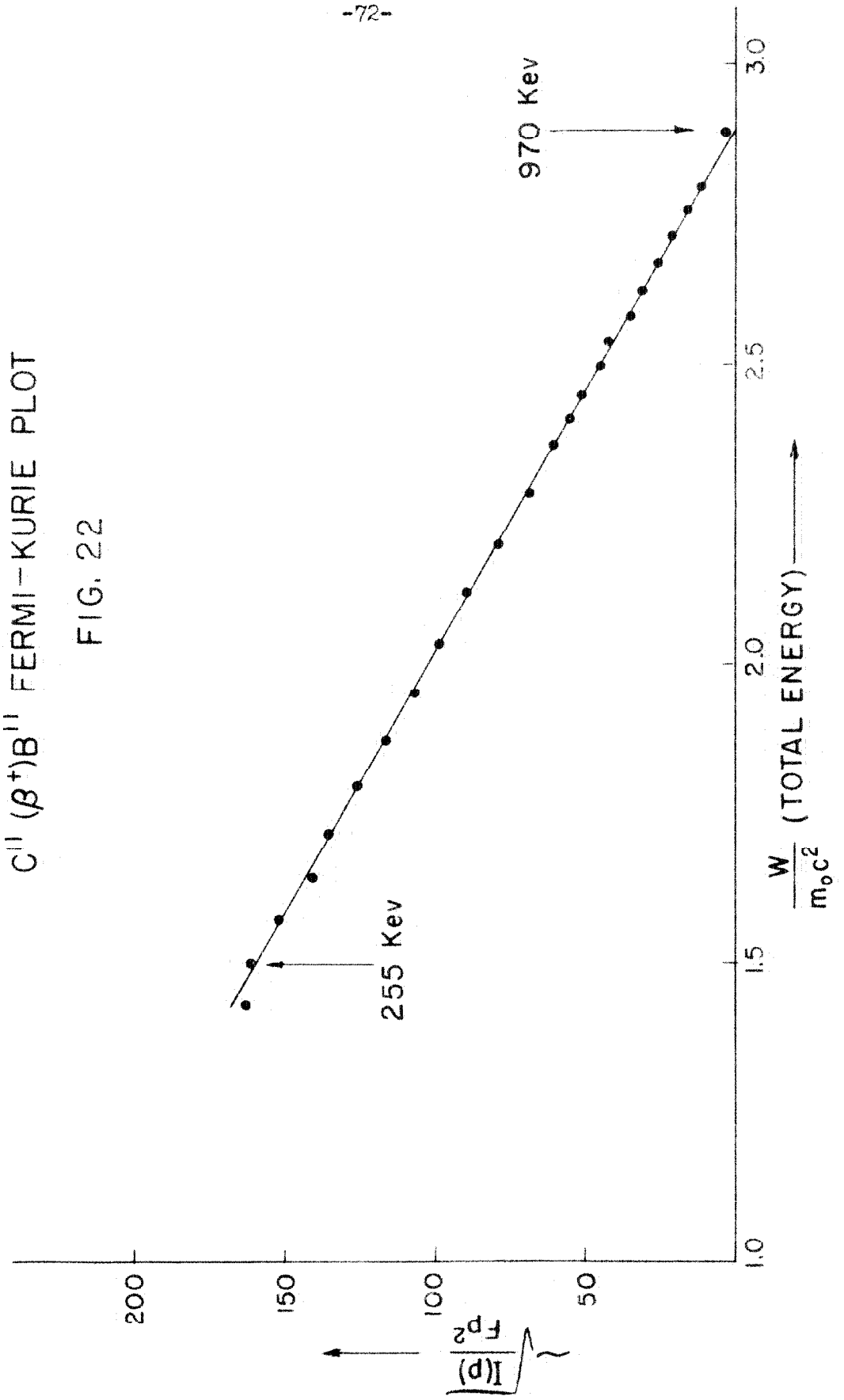
$C^{11}(\beta^+)B^{11}$ FERMI-KURIE PLOT
970 Kev
255 Kev
$\sim \sqrt{\frac{I(p)}{F_{p^2}}}$
$\frac{W}{m_o c^2}$ (TOTAL ENERGY)
200
150
100
50
1.0
1.5
2.0
2.5
3.0

FIG. 22

CONVERSION ELECTRONS FROM THE PROMPT AND DELAYED RADIATION ($O^{16}+d$)

FIG. 23

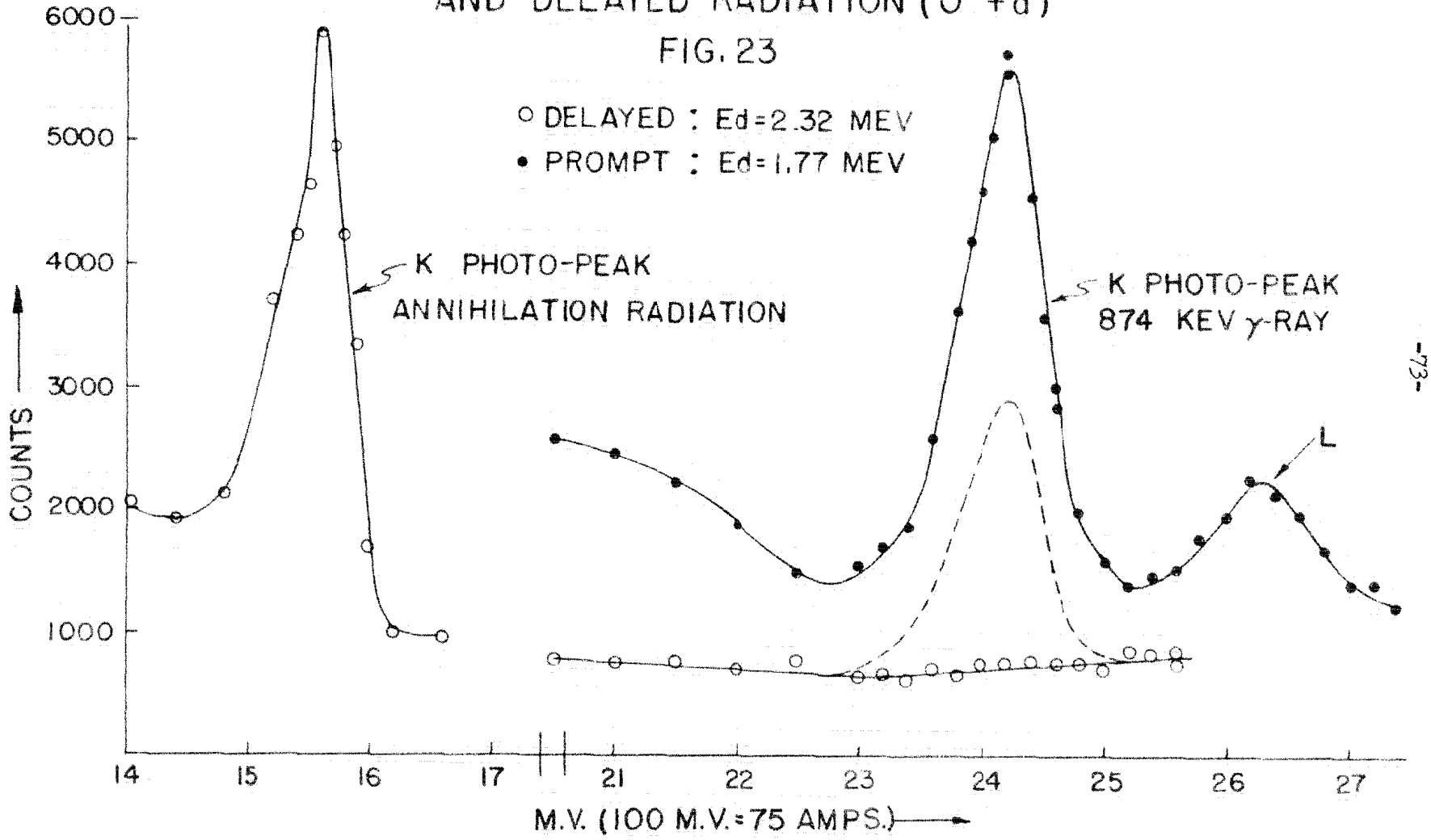

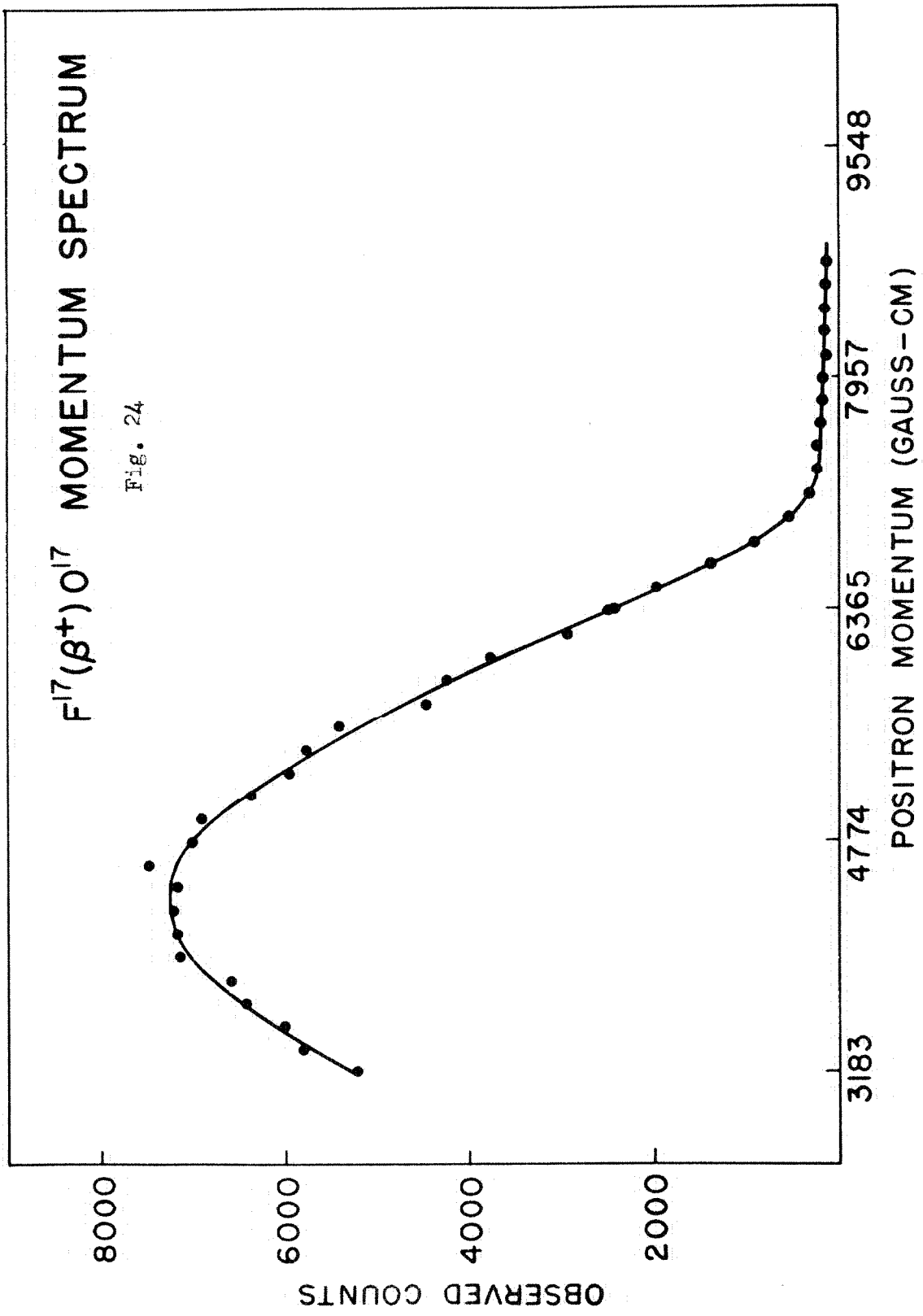
F17(β+)O17 MOMENTUM SPECTRUM
Fig. 24
OBSERVED COUNTS
8000
6000
4000
2000
3183
4774
6365
7957
9548
POSITRON MOMENTUM (GAUSS-CM)

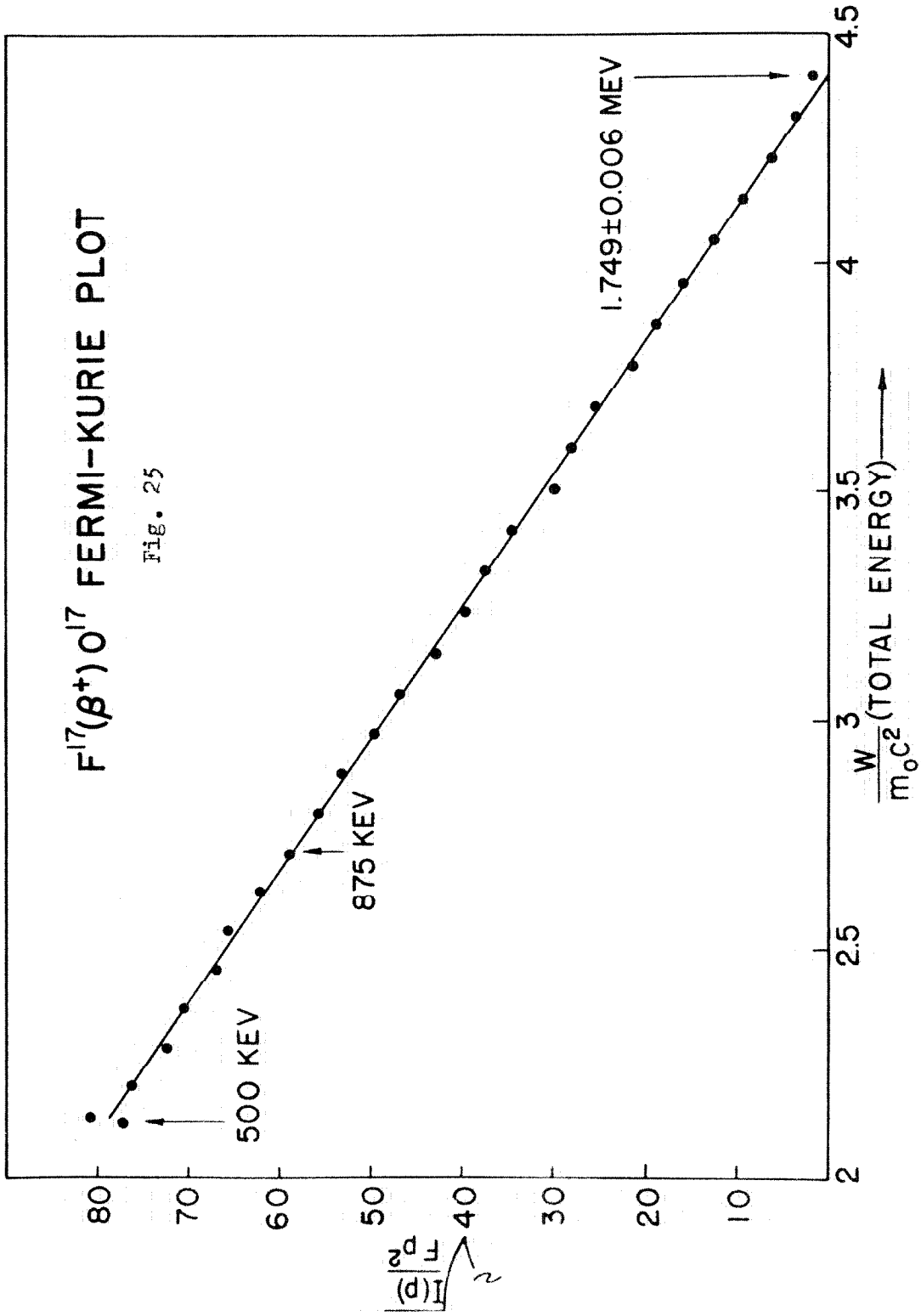
F17(β+)O17 FERMI-KURIE PLOT
500 KEV
875 KEV
1.749±0.006 MEV
I(p)/F p2
W/m0c2 (TOTAL ENERGY)
80
70
60
50
40
30
20
10
2
2.5
3
3.5
4
4.5

Fig. 25

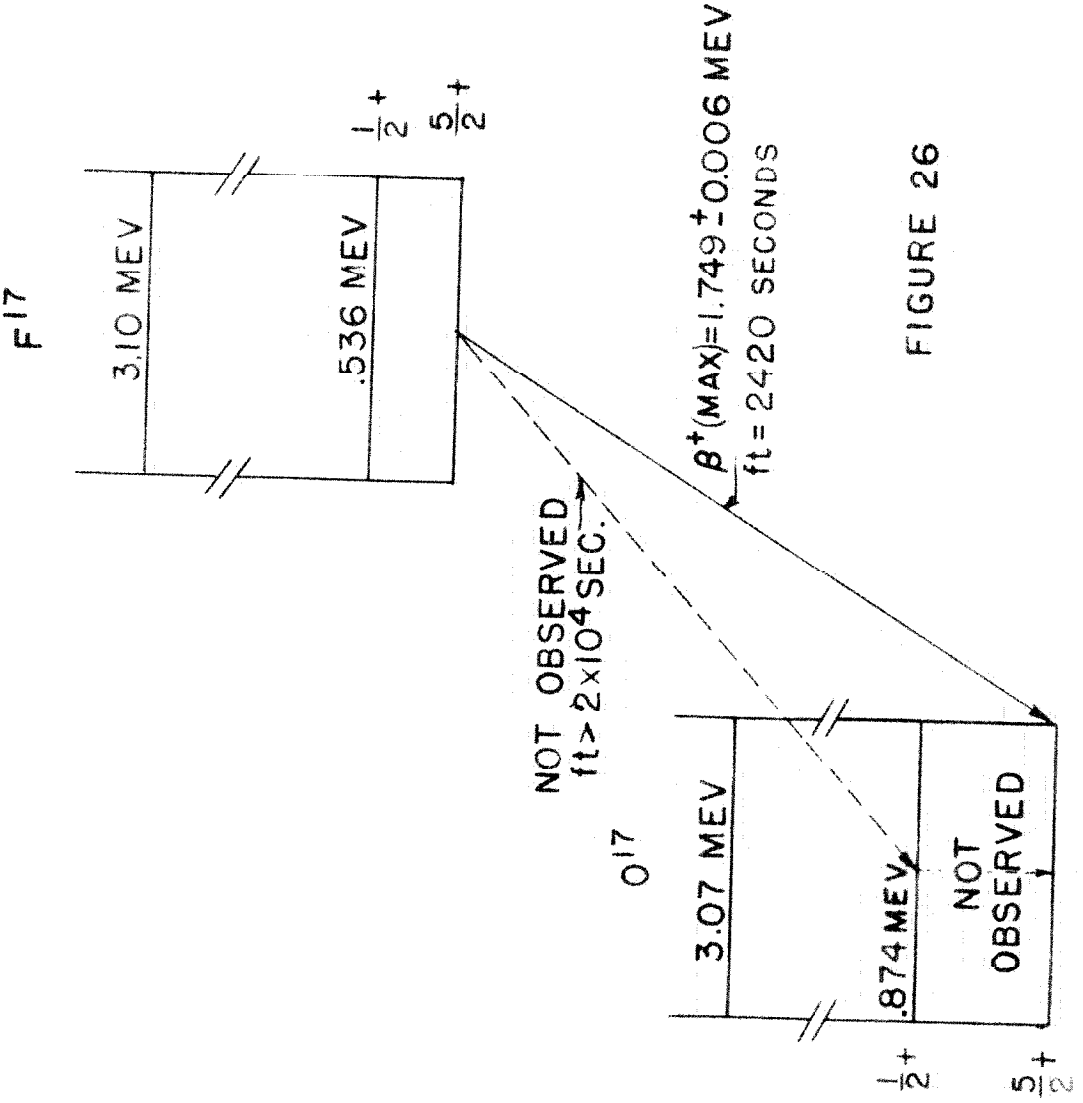
F17
3.10 MEV
.536 MEV
1/2+
5/2+
β+(MAX)=1.749±0.006 MEV
ft = 2420 SECONDS
NOT OBSERVED
ft > 2x10⁴ SEC.
O17
3.07 MEV
.874 MEV
NOT OBSERVED
1/2+
5/2+

FIGURE 26

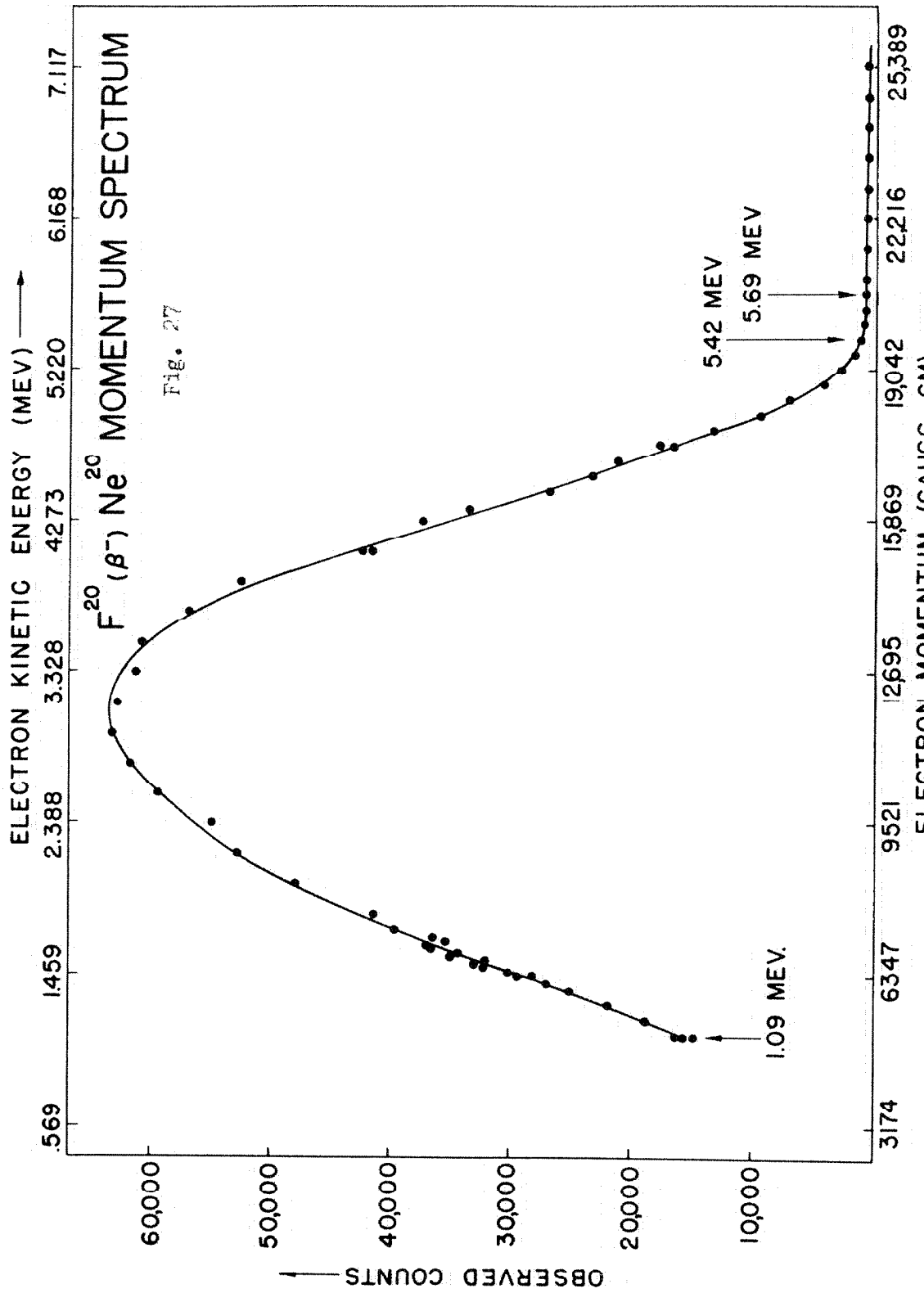
$F^{20}(\beta^-)Ne^{20}$ MOMENTUM SPECTRUM
Fig. 27
ELECTRON KINETIC ENERGY (MEV) ⟶
.569
1.459
2.388
3.328
4273
5.220
6.168
7.117
ELECTRON MOMENTUM (GAUSS-CM) ⟶
3174
6347
9521
12,695
15,869
19,042
22,216
25,389
OBSERVED COUNTS ⟶
60,000
50,000
40,000
30,000
20,000
10,000
1.09 MEV.
5.42 MEV
5.69 MEV

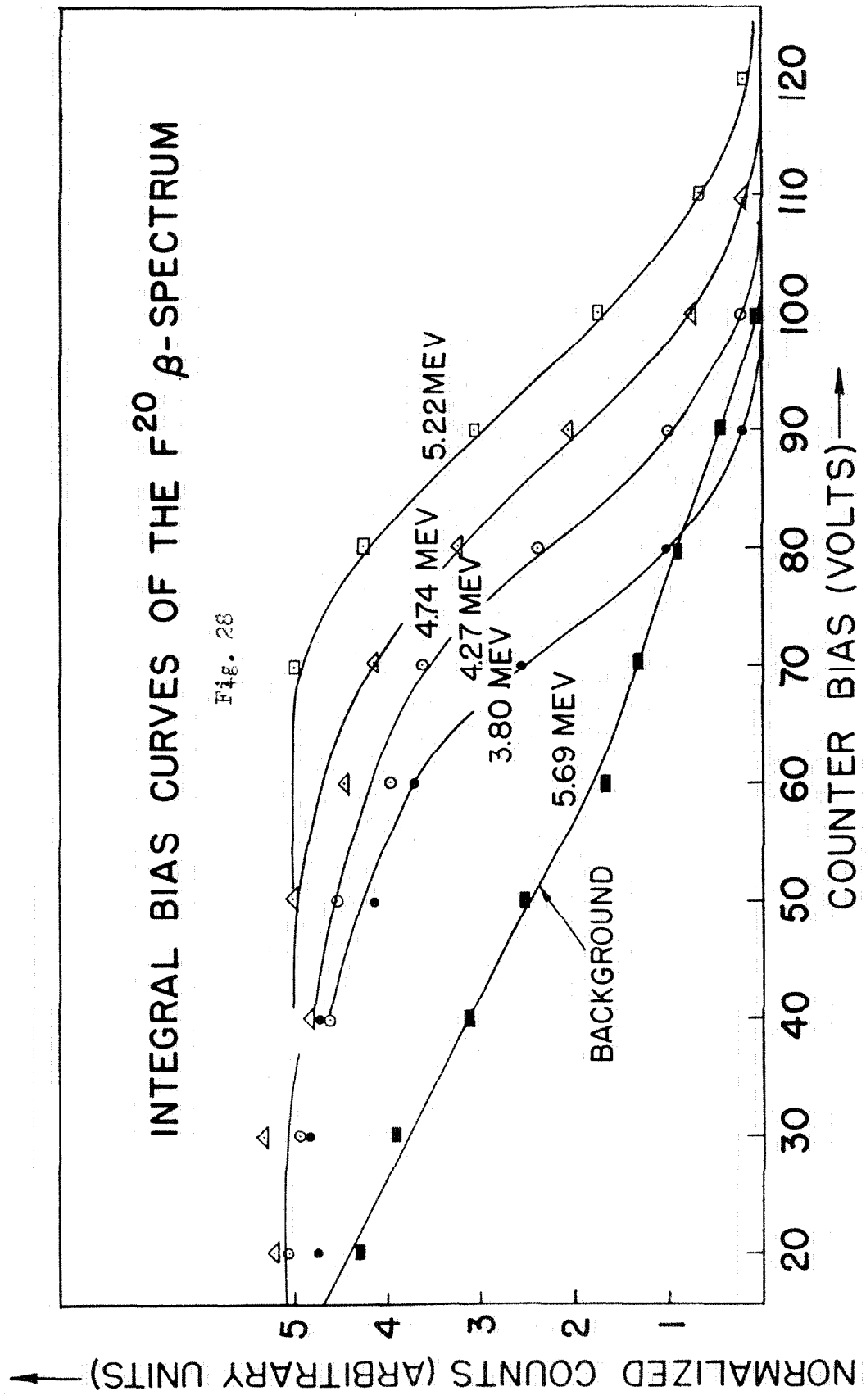
INTEGRAL BIAS CURVES OF THE $F^{20}$ $\beta$-SPECTRUM
5.22MEV
4.74 MEV
4.27 MEV
3.80 MEV
5.69 MEV
BACKGROUND
NORMALIZED COUNTS (ARBITRARY UNITS)
COUNTER BIAS (VOLTS)
1
2
3
4
5
20
30
40
50
60
70
80
90
100
110
120

Fig. 28

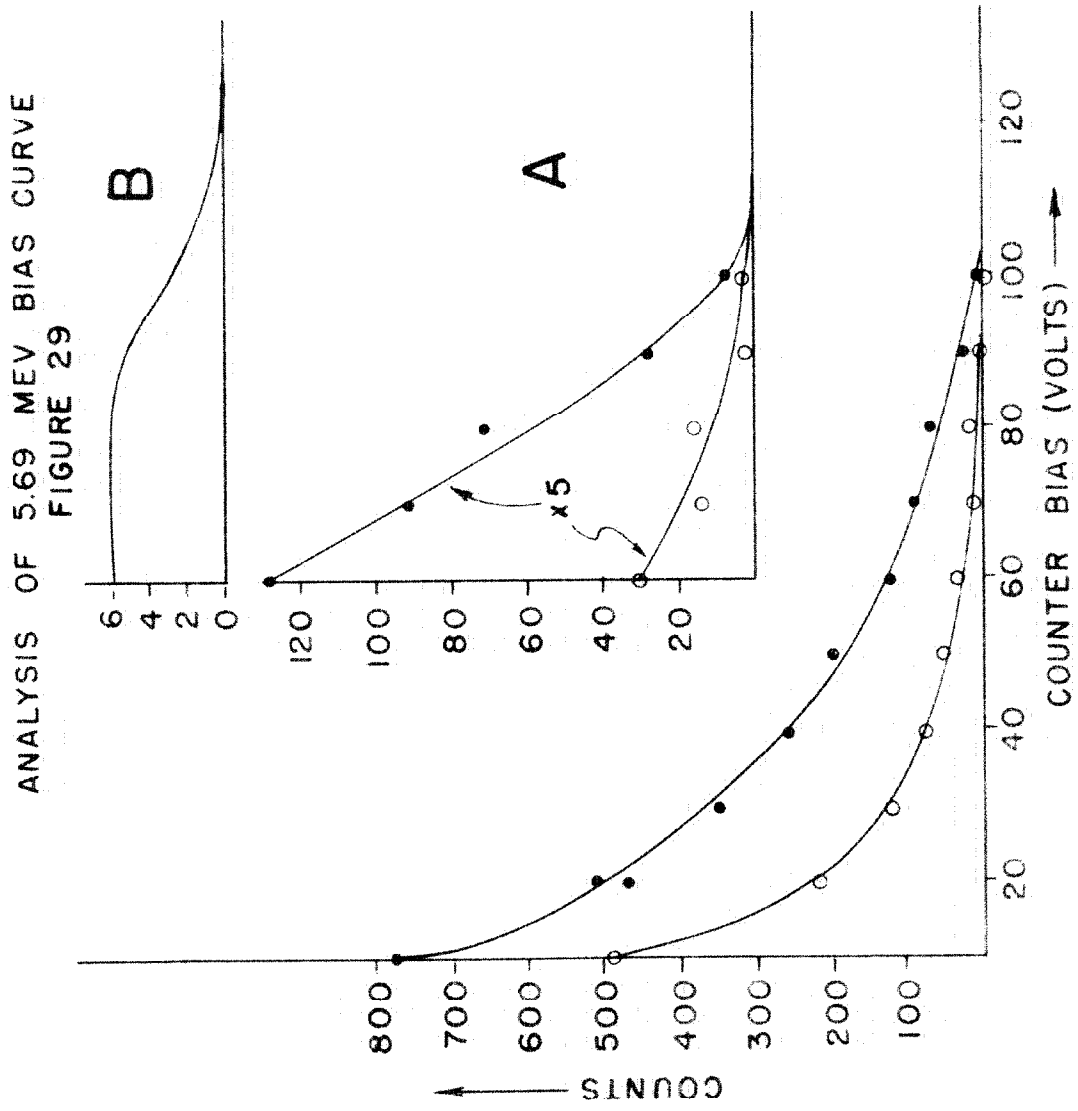
ANALYSIS OF 5.69 MEV BIAS CURVE
FIGURE 29
B
A
x5
COUNTS
COUNTER BIAS (VOLTS)

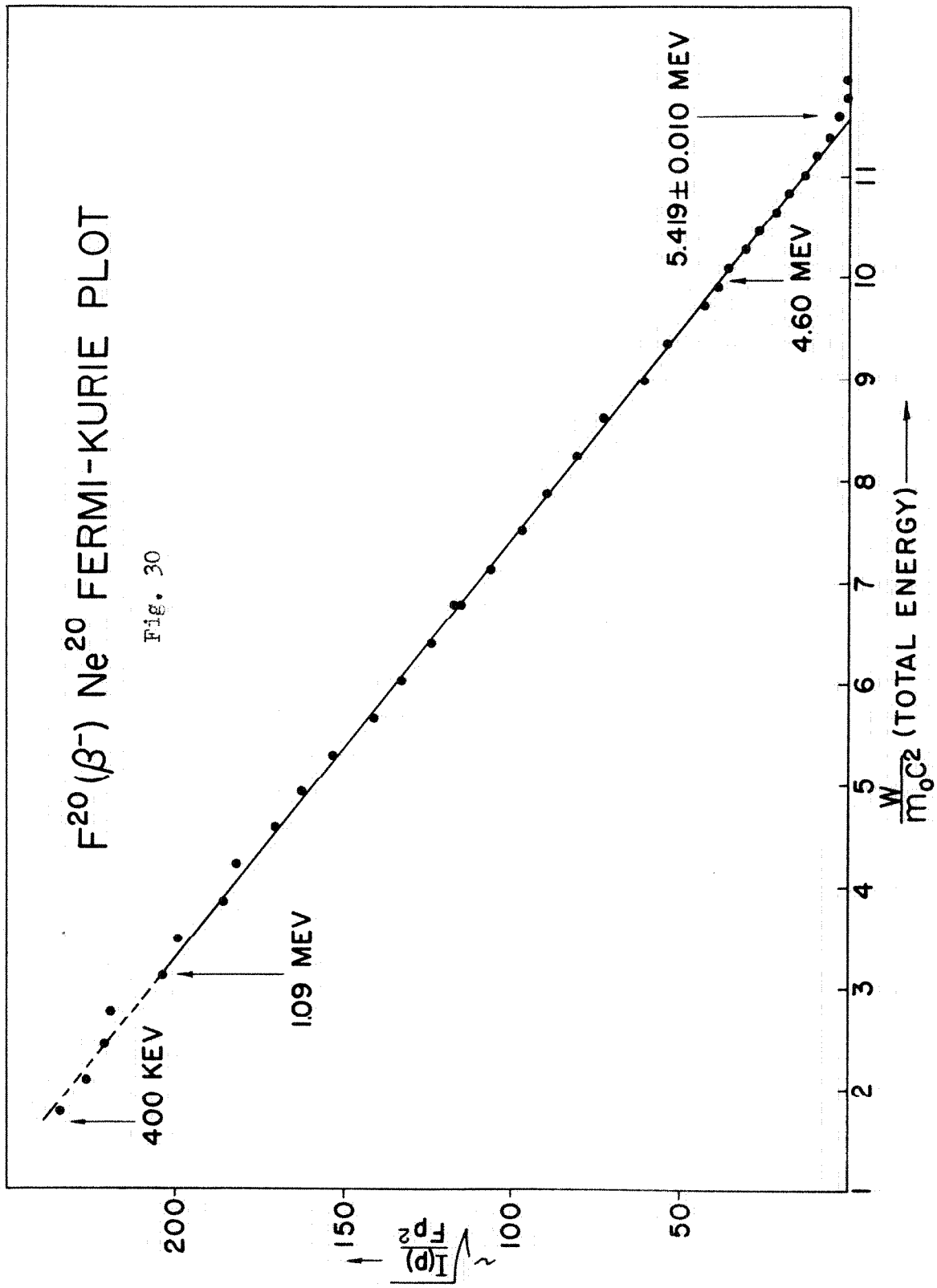
F20 (β-) Ne20 FERMI-KURIE PLOT
400 KEV
1.09 MEV
4.60 MEV
5.419 ± 0.010 MEV
200
150
100
50
1
2
3
4
5
6
7
8
9
10
11
W/m0C2 (TOTAL ENERGY)
~ √I(p)/Fp2

Fig. 30

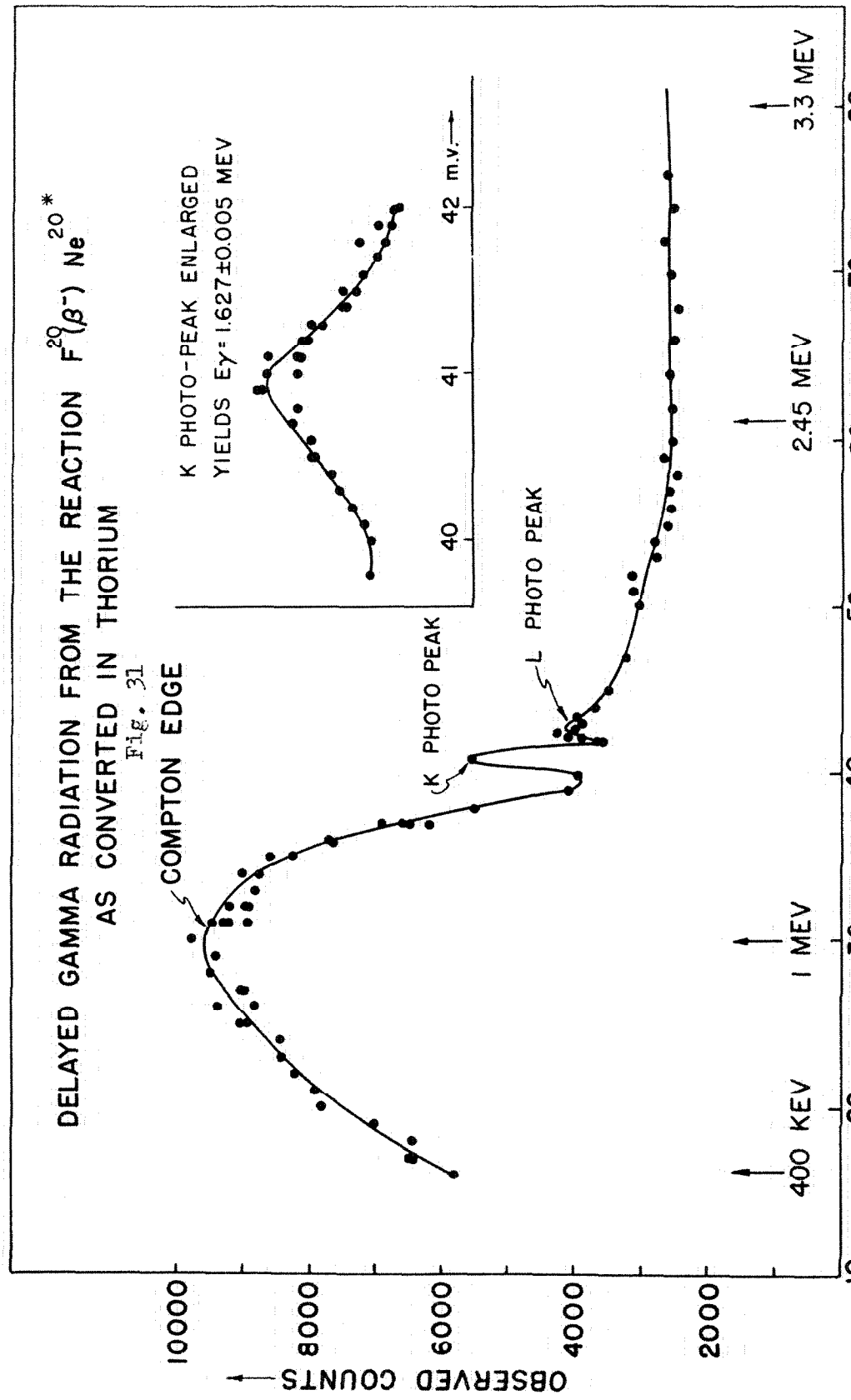
DELAYED GAMMA RADIATION FROM THE REACTION $F^{20}(\beta^-)\ Ne^{20*}$
AS CONVERTED IN THORIUM
Fig. 31
COMPTON EDGE
K PHOTO PEAK
L PHOTO PEAK
K PHOTO-PEAK ENLARGED
YIELDS Eγ = 1.627±0.005 MEV
40
41
42 m.v.
400 KEV
1 MEV
2.45 MEV
3.3 MEV
OBSERVED COUNTS
SPECTROMETER SETTING (M.V.)
10000
8000
6000
4000
2000
10
20
30
40
50
60
70
80